Master of Science Thesis

Load Transfer Investigation of a Hybrid Doubler Repair

Florian Vandenberk

Faculty of Aerospace Engineering · Delft University of Technology

TU Delft Delft University of Technology

Load Transfer Investigation of a Hybrid Doubler Repair

Master of Science Thesis

For obtaining the degree of Master of Science in Aerospace Engineering
at Delft University of Technology

Florian Vandenberk

9 January 2015

Faculty of Aerospace Engineering · Delft University of Technology

The work in this thesis was supported by Airbus GmbH. Their cooperation is gratefully acknowledged.

Delft University of Technology
Faculty of Aerospace Engineering
Department of Aerospace Structures and Materials

GRADUATION COMMITTEE

Dated: 9 January 2015

Chair holder:

prof. dr. ir. R. Benedictus

Committee members:

dr. ir. R. Alderliesten

dr. ir. R. Starikov

dr.ir. C. Kassapoglou

Reader:

ir. R. Heron

Summary

The goal of this thesis was to analyse the load transfer capability of a hybrid doubler repair by comparing a finite element solution to simplified internal Airbus tools, focusing on the effect on the fatigue life. This was done using a combination of commercial finite element tools (Abaqus) and internal Airbus stress tools. Since it is too time-consuming to perform every time a finite element investigation for each repair justification, an analytical method was developped to perform the justification.

The first step was to create a finite element model using Abaqus which was used to observe the influence of different parameters on the load transfer from the original structure to the doubler repair. It was observed that due to hybrid thermal effect which occured in all considered load cases with temperature difference, the most critical fastener hole was located at the edge of the doubler. In the past with a non-hybrid configuration (metallic skin with a metallic repair) the most critical location was located around the cut-out. This showed the great importance of the thermal stress on the location of the critical hole. Another observation was that the influence of the load transfer from the original structure to the repair was limited to the longitudinal stress direction. Therefor only a Load Increase factor should be applied on the longitudal component.

The outcome of the finite element model is compared to different simplified Airbus models (one-dimensional & two-dimensional stripe models and a simplified analytical equation). Here it was seen that the Airbus models are more conservative leading to higher Load Increase Factors than the finite element model. The simplified analytical equation which is only based on load fluxes and stiffness ratio's showed a bad correlation to the finite element solution. It was observed that the best match with the finite element model was reached with the two-dimensional Airbus static model.

Based on the correlations which were found in the finite element study and which were confirmed using the Airbus internal models, it was shown that a new analytical equation can be set-up for estimating the load transfer based on different loading and geometrical parameters. This analytical equation has been tested for three cases, where the transferred forces and the fatigue life has been calculated using the new analytical Load Increase Factor in combination with the Airbus fatigue model and the outcome is compared to the finite element model.

For the three analysed cases, a good correlation was found, though the Airbus fatigue model always lead to more conservative results than those found using the finite element solution. This means that the analytical equation can be used to estimate the Load Increase Factor. Another advantage of using the Airbus tool is the possibility to extract the maximum bore hole stresses, which allow to calculate directly the fatigue life of the metallic doubler. Since this module is already used for the justification of metallic repairs on metallic fuselages, it is therefor already known by the users and thus can be directly used within Airbus.

Table of Contents

List of Figures

List of Tables

List of Symbols

Symbol	Name	Unit
a	Fastener Depending Coefficient	[-]
b	Joint Depending Coefficient	[-]
f	Conjugate Vector	[-]
k	Stiffness Ratio	[-]
t	Thickness	mm
D	Fastener Diameter	$[mm]$
E	Modus of Elasticity	$[MPa]$
F	Force	$[N]$
F	Flux	$[\frac{N}{mm}]$
K	Stiffness Matrix	$[MPa]$
K	Stiffness	$[\frac{N}{mm}]$
L	Length	$[mm]$
N	Fatigue Life	$[Flights]$
R_x	Rotation around x-axis	[rad]
R_y	Rotation around y-axis	[rad]
S	Fastener Section Area	$[mm^2]$
T	Temperature	$[°C]$
T_z	Translation over z-axis	[-]
V	Volume Fractions	[-]
α	Linear Coefficient of Thermal Expansion	$[\frac{1}{°C}]$
δ	State Vector	[-]
ρ	Density	$[\frac{kg}{m^3}]$
$sigma$	Stress	$[MPa]$
Δ	Difference	[-]

Subscripts

c	Combination of Volume Fractions
n	Element Number
t	Thickness
x	Longitudinal Direction
xy	Shear Direction
y	Hoop Direction

I	Initial Node Force Vector
M	Mechanical Force Vector
T	Temperature

Acronyms

Al	Aluminium
CFRP	Carbon Fibre Reinfored Plastics
DOF	Degrees of Freedom
FC	Flight Cycles
FEA	Finite Element Analysis
LIF	Load Increase Factor
NDT	Non-Destructive Testing
SRM	Structural Repair Manual
Ti	Titanium
XWB	Extra Wide Body

Preface

On 20 August 2013, I started a new chapter in my life: I moved from my combined living place Delft, The Netherlands (weekdays) and Geel, Belgium (weekends) to Hamburg for a new adventure. I started my compulsory internship under Roman Starikov and Renaud Heron to help them with the analysis of fatigue and damage tolerance for skin repairs on the A350XWB. This was a great experience, in which I learned a lot from different stakeholders within Airbus. At the end of my internship, I was offered by Roman a place within the team to continue with a thesis, the result which you are now reading. It was a wonderfull experience where I learned to deal with time management and priorization between my thesis topic and other Airbus topics, which was personally sometimes hard.

I would like to start thanking my supervisors Roman Starikov and Renaud Heron at Airbus, but also René Alderliesten at Delft University. Without their continious supervision and advice, it would have been impossible to create this thesis. Next to this, I want to thank the other members of my graduation commitee, Rinze Benedictus and Christos Kassapoglou. Also I need to thank Regina Tange and Renaud Heron for proof reading this work.

Secondly, I also need to thank my parents, my sister Diede, my girlfriend Maja and the rest of my family, for all their support. Even though I was in Germany, I could always rely on them and they always tried to motivate me to give the best of myself. Thanks!

A special appreciation needs to go to Rik (Richard) Adema. I already knew him before I came to Hamburg, as a teaching assistant in structural subjects, as fencing trainer on sabre, as a nice social partner after training, but mainly as a friend. I would really like to thank him for all support during the past years, from the possibility to sleep at his place the first weeks in Hamburg, for all nice evenings we had together, for all trainings and after-trainings (in Delft and Hamburg) and for all nice conversations (work and non-work related). Rik, thanks for being such a good friend!

Next on my list are my Airbus collegues; my direct ESKNSR-team collegues Alexandre Bleneau, Jean-Michel Morand, Lars Aberspach, Helen Williams, Romain Coemet, Thomas Hobbiebrunken & Julien Le Coq and all interns, thesis- and working students of the past months: Marcus, Jean-Noel, Adrien, Abedin and ofcourse Diletta! Secondly, all collegeas of other teams where I had interactions with, Gianluca for his help and advice on the parametric in-

vestigation and all other fatigue topics; Lisa and Sergio for answering all questions regarding the SRM-design principles; Thomas Beumler for the nice talks about the wonderful world of Glare.

I will never forget my time and the people in Delft: all members of Delft Fencing Club and in special Noud, Serge, Boudewijn and Yasmine with who I had great trips to Rotterdam; the wonderful conversations I had with my roommates Bram and Gert-Jan; my other friends in Delft with who I had a wonderfull time during lectures, projects and of course in the evenings especially Frederik; all co-board members of Enlightness; Gillian Saunders for the good talks and her advice; Vincent Brugemann and Nando Timmer and all my collegue student-assistants, because they gave me the possibility to taste the feeling to sit on the other side of the desk.

For my time in Hamburg, a big thanks need to go to all people of ETV Fencing Hamburg and especially to Paul, Stephan, Gesche, Kim, Chris and Olaf for giving me a wonderfull time and accepting me that quickly in an already long-existing friendship. I cannot forget my Hamburger co-interns, known as the "Hamburger Hooligans" for having great evenings and parties at home or at the famous Hamburger Reeperbahn.

And for all my other friends, family and those I forgot to mention, but who supported or contributed to this thesis, thank you.

Florian Vandenberk
19 December 2014
Geel, Belgium

"Flying is so many parts skill, so many parts planning, so many parts maintenance, and so many parts luck. The trick is to reduce the luck by increasing the others."

— *David L. Baker*

Chapter 1

Introduction

From the start of aviation, aircraft design and repairing aircraft go hand-in-hand. Before the first flight of the Wright brothers, a trial ended in a loose of control of the aircraft, damaging a wing. Luckily, it could be repaired within three days and on December 17, 1903 the first controlled, powered and sustained heavier-than-air human flight took place [27]. Since that time, aviation changed drastically. Over the years, aircraft became larger, could fly further and could carry more passengers. This could only be possible by a change of materials: from wood and line in the time of Wright brothers, to metals, fibre metal laminates and more and more composites over the last years. However, just as in the early days, aircraft still need to be repaired and all these different materials need different repair approaches.

In 2006, Airbus introduced a new fuselage concept, mainly made of CFRP (Carbon Fibre Reinforced Plastics). Just as with the Wright brothers, at one point, the airliner needs to repair the fuselage. The repair leads to a restoration of the original load carrying capability, which needs an in-depth load transfer analysis. One of the possible skin repair concepts of a composite fuselage is the use of metals, e.g. Aluminium and Titanium. However, this hybrid configuration leads to a more complex load transfer, due to the difference in stiffness of the different elements, the stiffening elements already present (stiffeners) and the introduction of thermal stresses due to the different thermal expansion coefficients of the materials. In the past when a hybrid configuration was applied, the hybrid influences were neglected or the repair was oversized. But now that more and more parts are made of composites, a detailed justification is needed. The goal of this thesis research is to analyse the load transfer capability of a hybrid repair by comparing a finite element analysis to simplified internal Airbus tools.

The first step was to have a look at the background of the problem, which is done in Chapter 2, where the available literature on the subject is summarised. Further, a more detailed motivation of the problem is given, explaining the reasons why a detailed analysis of a hybrid repair is needed. After this, the problem is fully described and the analysis could start, which is visualised with a flowchart, in Figure 1.1.

To start the analysis a detailed model of a hybrid doubler repair was created using finite element software, in this case Abaqus. The model was runned for different parameters, such as material, cut-out size and doubler thickness. This model gives a good overview of the general behavior of a hybrid doubler repair in different situations. This all is presented in Chapter 3. The outcome of this study for different cases is a Load Increase Factor, which describes the amount of load which is transferred from the stringer to the repaired skin.

It is impossible to create, run and analyse each repair justification with such a complex finite element model. Therefor, simplifications need to be introduced. Within Airbus, different models containing these simplifications already exist. So the next step (Chapter 4) is to run the different configurations using these simplified models and to see the differences in the behavior and to get an idea of the level of conservatism of the different models.

However, this research aims to go even one step further, namely to create an analytical equation which is based on the results of the finite element model (Chapter 5). Using this equation, it should be possible to have a reliable and fast way of calculating the load transfer.

In the last chapter, Chapter 6, the main conclusions and recommendations for further research into this topic are provided.

All the work presented in this document is subjected to a non-disclosure agreement, signed between Airbus and Delft University of Technology, which can be found in Appendix A.

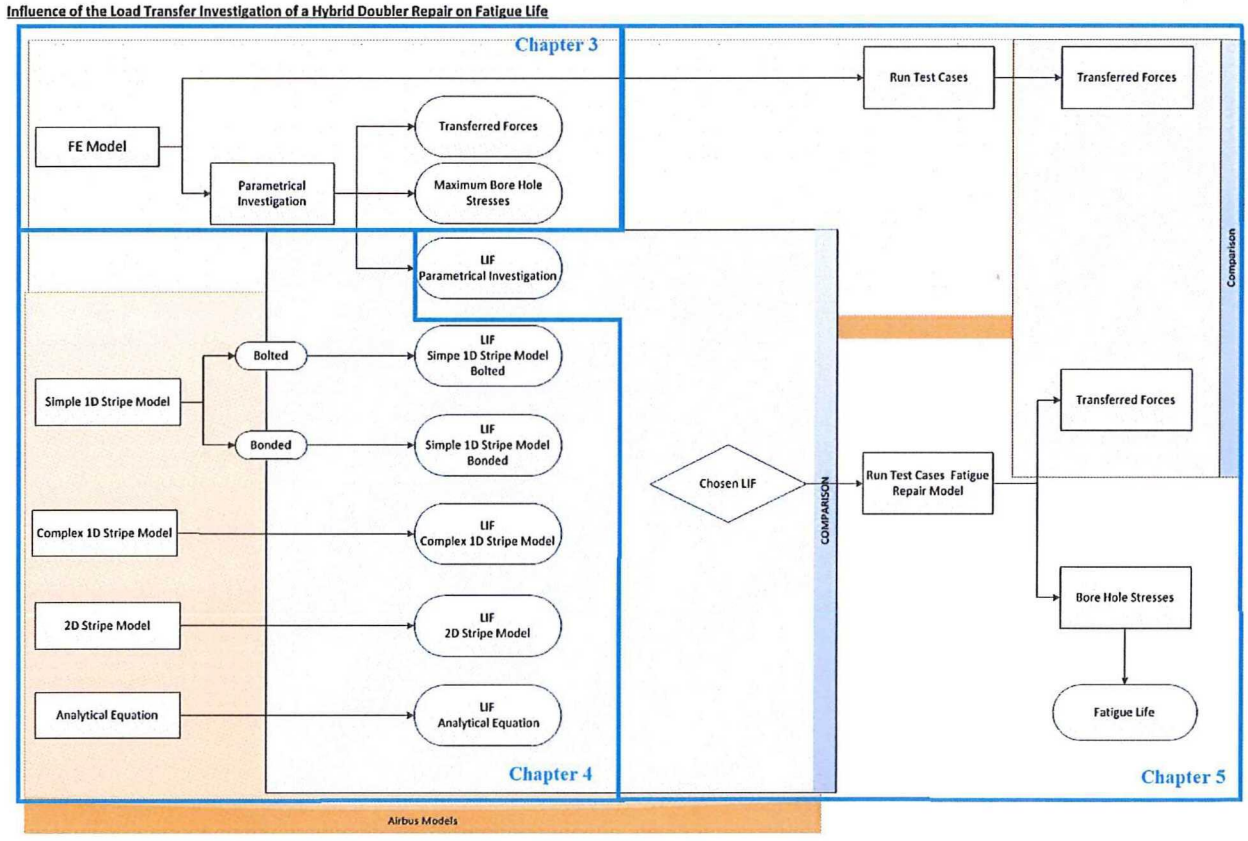

Figure 1.1: Outline of Thesis

Chapter 2

Background and Motivation

Already from the early days of flight, the question is not only how to design an aircraft, but also how to maintain and keep them in the air, so that ground- and maintenance times are reduced. To reach this goal the aircraft needs to undergo regular maintenance which includes structural repairs. Over the past decades, the service life of aircraft is extended for economic reasons, which increases the need of maintenance and the application of repairs. It is foreseen that in the near future the service lives will be extended even more, as illustrated by the initiation of different new life extension programs at all major aircraft manufacturers for existing aircraft programs. [3]

In the history of aviation, different materials (such as wood, different metallic alloys, composites...) are used in the aircraft industry. From the early 1970s, composites were introduced on the airframe. An overview of this development is given in Section 2.1.

The reasons for a shift in material usage are diverse. In Section 2.2 the different properties of CFRP (Carbon Fibre Reinforced Plastics) are described, with a main focus on the mechanical properties, but also on the advantages and disadvantages of the use of composite materials in aerospace structures. One of the repair techniques of these composite materials is to perform a repair with metallic materials, just as was done with metallic structures and introduces hybrid repairs on the airframe.

Repairs of composite structure which can be applied during the life of the airframe also need to be analysed and justified. This chapter focuses on one of the more frequent applied structural repairs, namely a skin repair using an external patch (doubler repair). The anisotropic properties of the composite skin yields to new considerations which should be made. This is due to the thermal effect and the difference in stiffness caused by the hybrid repair.

Section 2.4 discusses shortly how the fatigue life of a hybrid repair is justified and points out the main points where an improvement should be possible. All these steps are visualised in a flowchart, see Figure 2.1.

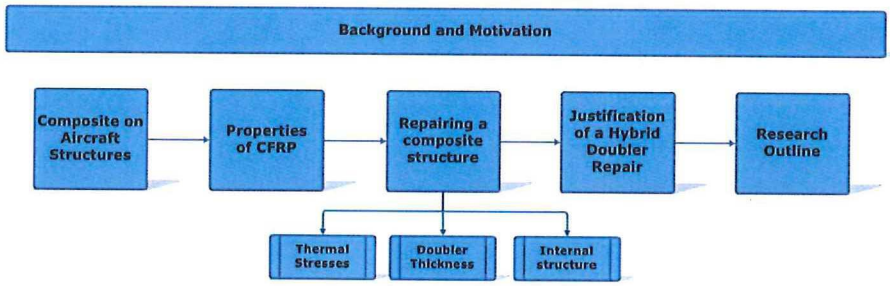

Figure 2.1: Flowchart of Chapter 2: Background and Motivation

2.1 Composite on aircraft structures

Due to the continuous technological development, many different materials are used these days within the aircraft industry. The first aircraft were produced out of wood and line and only had a limited service life [4]. Starting from World War 2, with the introduction of the first commercial aircraft, metals were used, such as Aluminium, Titanium and Steel. [4]

From the 1970s, composite materials are introduced on aircraft structures as can be seen from Figure 2.2. Airbus started on the A300 with some secondary structures made of composite, such as the fairings and the radome. In the next generation of aircraft, the use of composite material is increased, as can be seen in Figure 2.3. The technological development allowed that composite parts could become larger and bit by bit also large primary aerostructures could be made of composite material. In 2000, with the introduction of the A380, the inner-structure of the wing was produced out of composite (center wing box and wing ribs), see Figure 2.3. [2]

In 2006 Airbus presented the A350XWB concept, a long-range wide body aircraft family where most of the primary aircraft structure is made of composite material. The fuselage and wings of the A350XWB are made of composite stiffened skin panels, meaning a composite skin stiffened with co-bonded or co-cured composite stringers. In total, more than half of the structural weight is made out of CFRP (Carbon Fibre Reinforced Plastics). Figure 2.4 shows the percentage of the different materials used on the A350XWB and their location on the airframe. The properties and the main benefits of CFRP will be discussed in more detail in the following section.

2.2 Properties of Carbon Fibre Reinforced Plastics

Composites are one of the main materials for the airframe structure on the A350XWB. On this family, CFRP is used which is a polymer matrix composite material reinforced by carbon fibers. These carbon fibers can be oriented into different directions, leading to the typical anisotropic properties of CFRP, namely the directional strength properties of the material. The carbon fibers can be distributed to achieve the best load carrying capabilities for this part of the structure. This fiber placement optimization can lead to a better load carrying capability and a significant reduction in weight of the airframe structure compared to Aluminium,

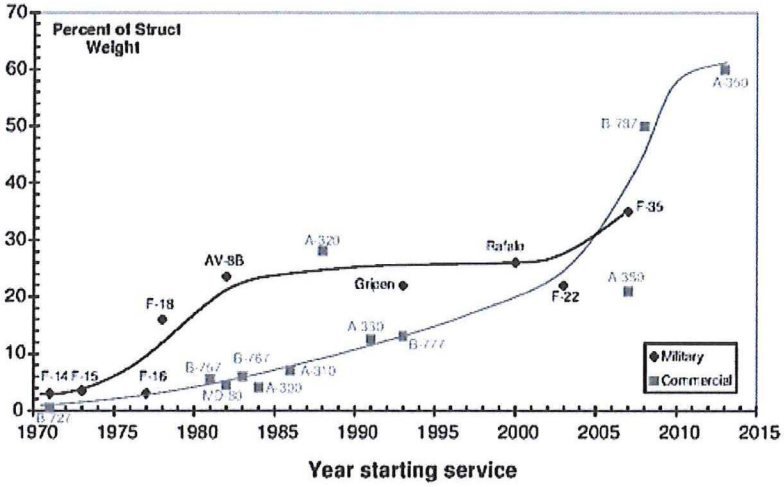

Figure 2.2: Overview of the use of composite on civil and military aircraft [11]

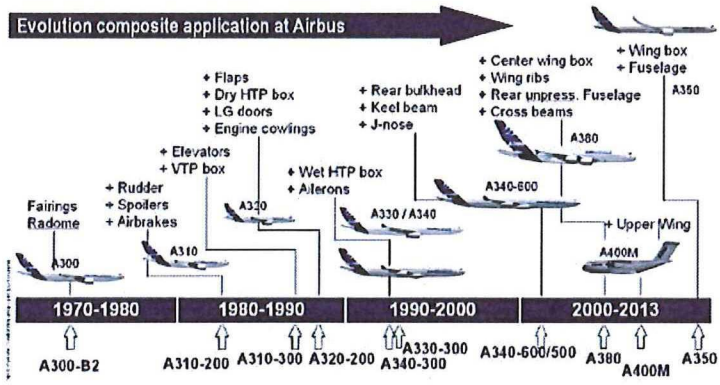

Figure 2.3: Overview of use of composite materials on Airbus aircraft over the years [6]

increasing the fuel efficiency of the aircraft. However, it should be noted that substantial weight savings are only possible through the judicious use of composite material. The selection of an optimum composite material depends mainly on the application requirements in terms of stiffness and loading type. [21]

In addition to these fiber placement optimization possibilities, composites have a high stiffness-to-density ratio (E/ρ), which is shown in Figure 2.5 where a comparison is made between CFRP and Aluminium. It shows that the Young's modulus of the two materials is in the same range, but CFRP has clearly a lower density. However, when quasi-isotropic CFRP would be used, the benefits are much smaller, as can be seen also from Figure 2.5. For such a case, Aluminium performs much better than CFRP.

A second property which can be compared is the strength-to-density ratio (σ/ρ), as is shown in Figure 2.6 where the strength is plotted against the density for different material groups.

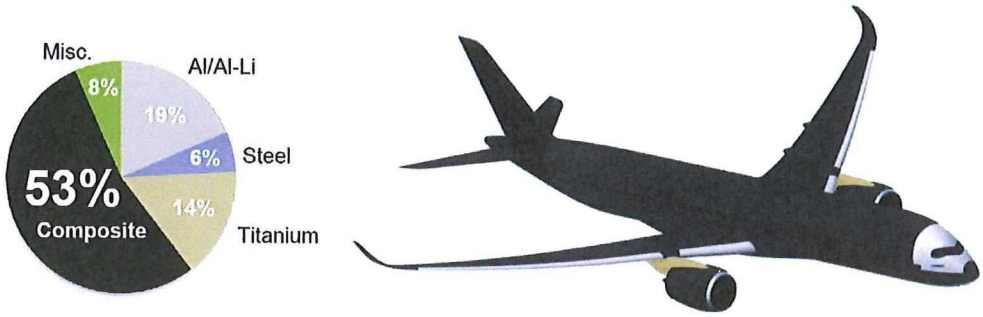

Figure 2.4: Overview of different materials used on A350-XWB [6]

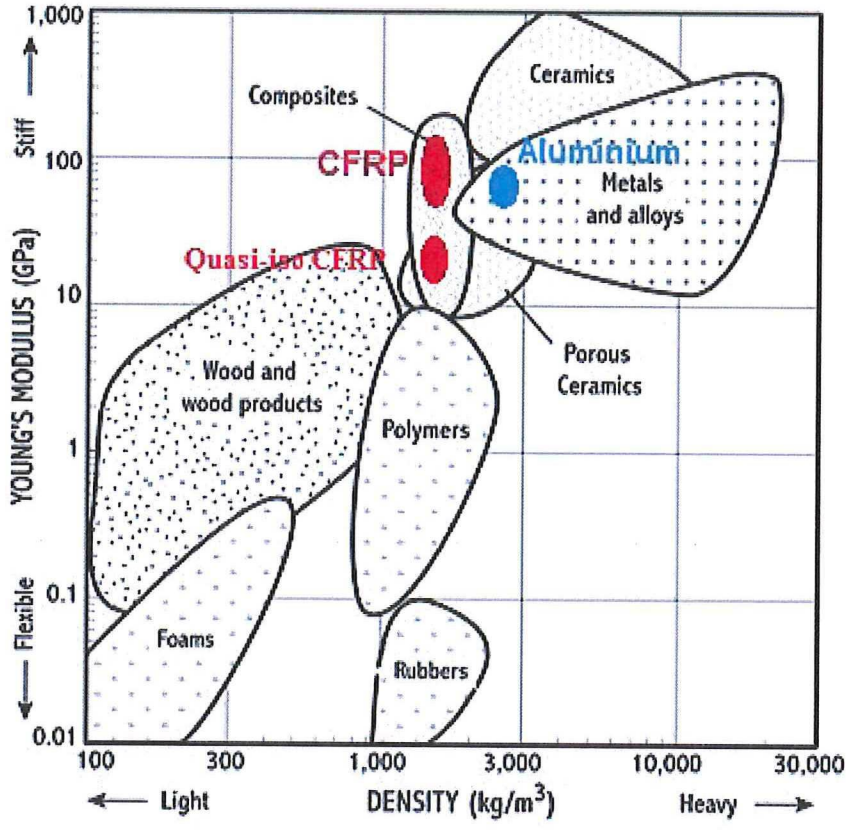

Figure 2.5: Young's Modulus [GPa] vs Density [kg/m^3] for different material classes [15]

From this figure, it can be seen that CFRP has a higher strength with respect to Aluminium and a lower density, leading to a lower weight in case that $\sigma_{ultimate}$ is the design driver. It should be noted although that in this plot it is assumed that the CFRP has a lay-up which represents a high strength composite.

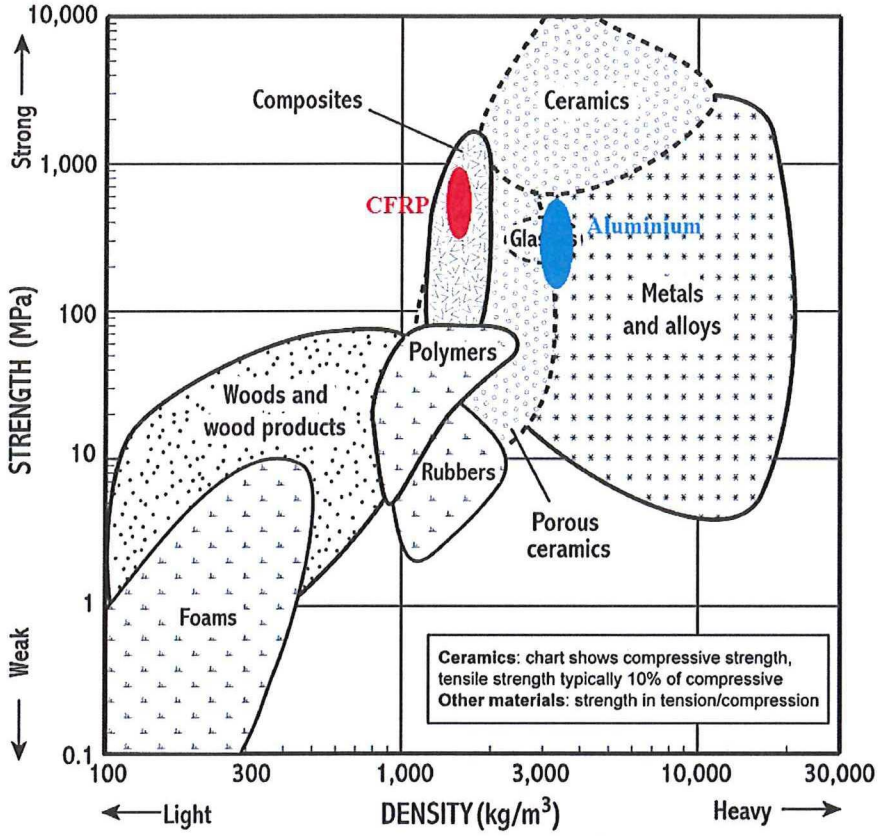

Figure 2.6: Strength [MPa] vs Density [kg/m^3] for different material classes [16]

In general it can be stated that the fatigue behavior of a composite is superior to metals for tension-tension loads due to its high fatigue endurance limit compared to the classical aircraft metallic alloys (Aluminium, Titanium). Figure 2.7 ,taken from [12], illustrates this behavior for a quasi-isotropic composite and Aluminium 7075-T6. Figure 2.8 shows the same behavior but then for a uni-directional composite. But since most structures are not purely loaded in tension, some composite show significant weakness in compression, shear and inter-laminar shear loadings after impact. It stays hard to compare this easily metallic and composite fatigue since the fatigue process for the two materials is different. In a metallic material, the crack initiates and propagates under repeated cyclic loading parallel to the original orientation, where in composites multiple types of damage can be present and interact. [12]

Composites and metallic material do have a different response on the environment. On one hand, composites do offer an excellent resistance to corrosion, although they do react galvanically with Aluminium when improper coupled. This can be mitigated during the design phase by proper design of the hybrid couplings between the metal and the composite [21]. Composites do respond on moisture (and humidity) in a different way. Moisture can diffuse

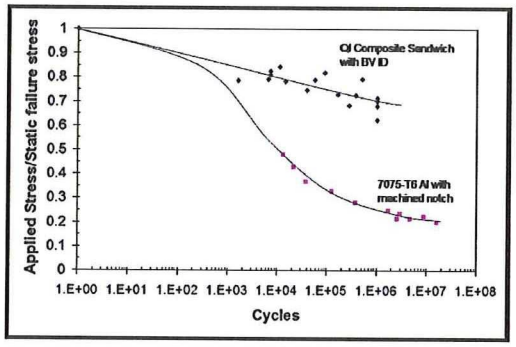

Figure 2.7: Fatigue behavior of quasi-isotropic composite and Alumunium 7075-T6 [12]

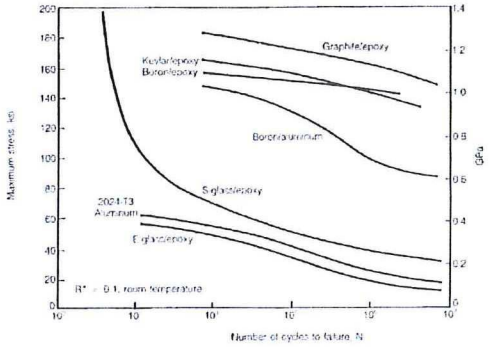

Figure 2.8: Fatigue behavior of uni-directional composites and Aluminium [21]

into into the composite, where it can degrade the fiber-matrix interfacial bonding, decrease the ultimate tensile strength and elastic moduli and can introduce microcracks in the matrix. [22] [23] [24]

However composites also have some disadvantages. One of the critical issues with composites is the high cost of production. Although the raw material costs are comparable to the classical aerospace alloys, the production costs are much higher. Also the use of a new material lead to different production and manufacturing processes, which gives the company a higher risk and cost increase.

A composite is mostly more brittle and thus more prone to damage than a metal. However, delaminations in a structure are allowed as long as thet do not grow in-service. In composite materials the visibility of the damages is harder than in a metallic structure where cracks can be spotted from the outside with simple visual inspection. The failure mechanisms in composite are more complex and therefor NDT (non-destructive testing) must be used mostly to find damages (such as delaminations). Therefor there is a chance that critical flaws and cracks may be undetected. [21]

Also when carbon fibres are cut, a fine dust of carbon fibre particles is easily released into the atmospehere. These fibres pose a risk since they are vulnerable for the skin und lungs, causing irritation. Therefor, during the cutting of the CFRP, special protection clothing, eye-protection, gloves and respiratory protection should be weared. [14]

A CFRP-structure requires an extra lightning strike protection since it is non-conductive. A lightning strike always seeks the available metallic paths, so a lightning strike protection in a composite is used by adding a fine mesh of copper. [21]
Due to this different behavior and the fact that composites as a main primary structural material is only applied since a couple of years, there is still only a basic knowledge about how to repair a composite structure. More details about the knowledge and challenges of repairing a composite structure can be found in the following section.

2.3 Repairing a composite structure

Repairs of an airframe are needed when potential failures during maintenance of functional failures (during operation) are detected. The goal of a repair is to restore the capability of the part to withstand the design ultimate loads, keeping in mind the location and function, such as aerodynamic smoothness. [20]

One of the standard repairs is a bolted skin repair using an external patch, see [18]. In the case of a metallic fuselage, the patch was made of the same material with a similar thickness for the skin at that location, to de-stress locally the skin and to increase the force flux going through the repair. However, this is not that straightforward for a composite fuselage since the CFRP-skin has anisotropic strength properties, leading to different skin stiffnesses in different loading directions.
Since the airliners already had the experience of repairing the metallic fuselage with metallic patches, it was decided that also a composite fuselage should be repairable with metallic patches. Using this approach, the airline manufacturers could use the same methods as was done in the past. However, the hybrid configuration of such a repair leads to extra points which should be considered, namely:

- the occurrence of thermal stresses due to the different thermal expansion coefficients.
- the determination of doubler thickness due to the anisotropic properties of the skin.
- the influence of the present stiffening structures.

These three points will be discussed shortly in the following sections.

2.3.1 Thermal stresses

When a material is loaded with a thermal load, the material changes its dimensions. In general, it can be stated that when the temperature increases, a material expanses and whereas the temperature decreases, the material will contract. For a homogeneous and isotropic material, the thermal expansion or extraction can be assumed to be linear, with the deformation described using following equation (from [10])

$$\Delta L = \alpha \cdot \Delta T \cdot L \tag{2.1}$$

where:

- α = linear coefficient of thermal expansion [1/°C].
- ΔT = change of temperature [°C].
- L = original length [mm].
- ΔL = change in length due to the temperature effect [mm].

Since the movement of the member is constrained in an external doubler repair by the rivets, thermal stresses occur and must be taken into account during the stress justification. In general, the behavior as described in Figure 2.9 can be observed for the effect of a pure mechanical load, a pure thermal load and a combined mechanical-thermal load for a uni-directional tensile or compressive loading. A doubler repair is a combination of a splice and a doubler since a cut-out will be modelled in the repair.

However a composite (in this case a skin with a specific lay-up) is a non-isotropic material and thus needs a different analysis since for every different lay-up of the composite a different thermal expansion coefficient exists. Here, the thermal coefficient is determined using the rule of mixtures, which is a weighted mean method used to predict the various properties of a composite material made up of continuous and uni-directional fibers. For thermal expansion, the rule of mixture is

$$\alpha_c = \sum_{n=1}^{\infty} V_n \alpha_n \tag{2.2}$$

where:

- α_c = combined thermal expansion coefficient.
- V_n = volume fractions of the phases.
- α_n = thermal expansion coefficients of each direction.

Another question which need to be answered are the temperatures which should be considered during the analysis. During the different stages of flight, the aircraft structure undergoes different temperature loadings. In [9] a research is done to the effect of thermo-mechanical loadings on Glare-laminates.

The research should be performed for the common service temperature range of a conventional airliner, which were found in [9]. The maximum static temperature in the skin can be around $85°C$, however for fatigue, the most detrimental temperatures are the negative temperature differences (around $-30°C$ to $-55°C$). These temperatures occur mainly during cruise-phase where the fuselage the dominating load is the internal pressure of fuselage skin in circumferential direction. For Aluminium it is known from literature (see references [25] & [7]) that the fatigue life of Aluminium with lower temperatures increases, as also can be seen from Figure 2.10. There, it can be seen that for increasing negative temperature, the number of cycles increases for the same crack length.

This provides additional conservatism in the analysis and during the full-scale testing. On the other hand when a hybrid structure is taken into account during full-scale testing, the benefit of the increase of fatigue life disappears to the extra thermal effect which is introduced on component level.

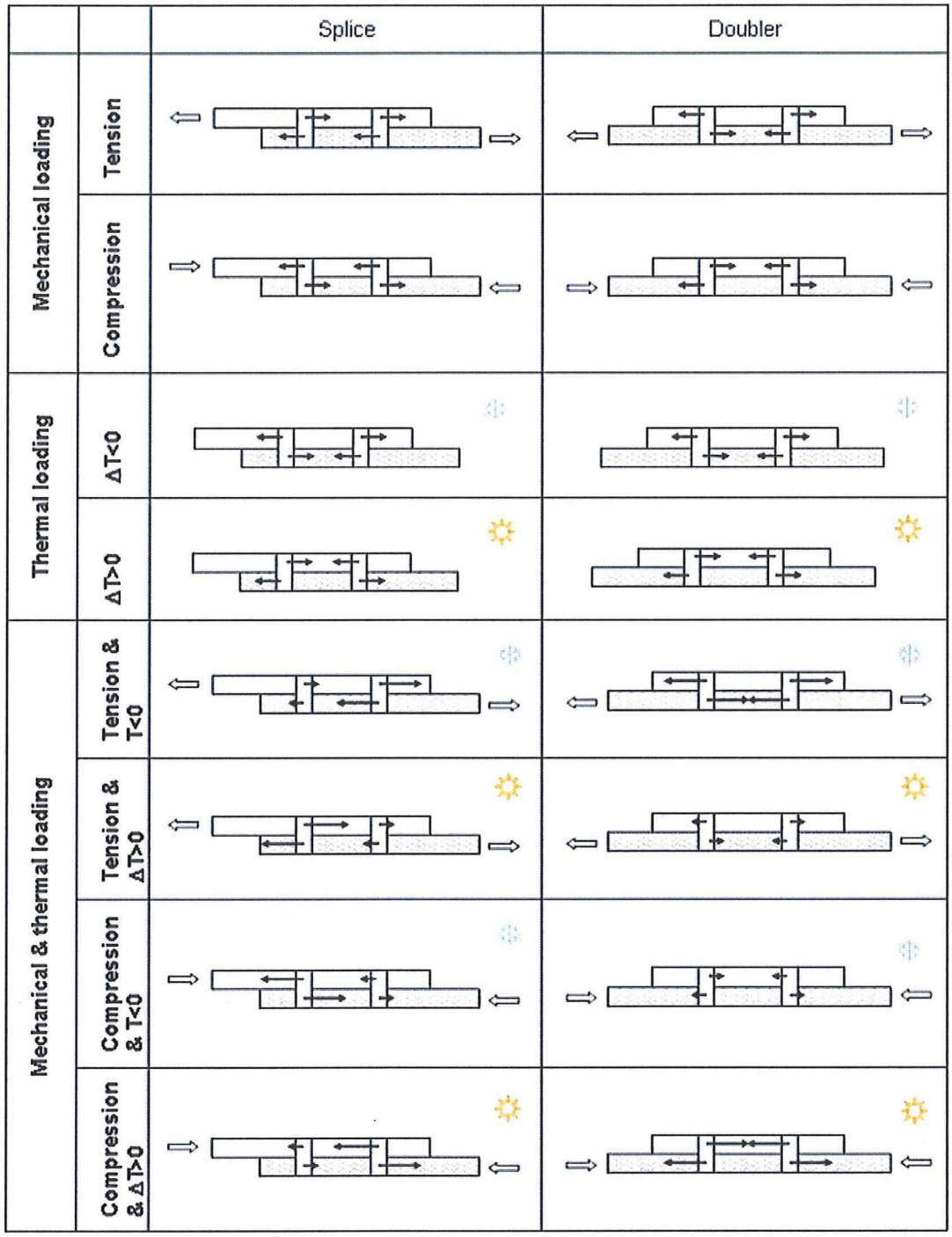

Figure 2.9: Thermo-mechanical effect on a hybrid joint for a splice and doubler configuration

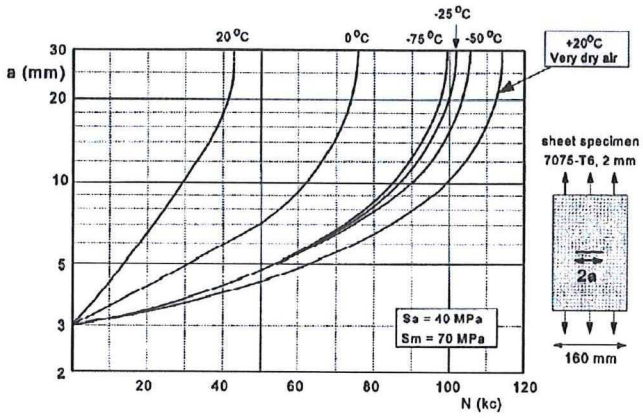

Figure 2.10: The effect of low temperatures on fatigue crack growth in specimens of an aluminium alloy [5]

2.3.2 Doubler thickness

The second point which needs to be discussed is the determination of the doubler thickness. Due to the anisotropic properties of a composite skin, it has a different stiffness in the different main loading directions. The doubler for the repair is sized based on an iso-stiffness approach. This means that the goal is to match the stiffness between the skin and the doubler patch, using following equation (from [10])

$$E_{mat1} \cdot t_{mat1} = E_{mat2} \cdot t_{mat2} \tag{2.3}$$

where

- E is the Young's Modulus of the material [MPa].
- t is the thickness of the material [mm].

The main advantage of an iso-stiffness approach is that the skin and the repair have the same stiffness and thus no major load attraction is expected to take place. However, due to anisotropic properties, this iso-stiffness condition can only be applied in one direction. The direction of the iso-stiffness requirement is mostly chosen in the main loading direction of the skin panel (longitudinal, hoop or shear loading). Due to this, it is expected that a load transfer takes place between the stiffened skin and the repair. This topic will be detailed in the following section.

2.3.3 Present stiffening structure

A third element which should be considered is the presence of stiffening elements within the structure, such as stiffeners. In the past, the stringers were mainly T-shaped and bolted to the fuselage. However, with the introduction of composite fuselages, also a different type of

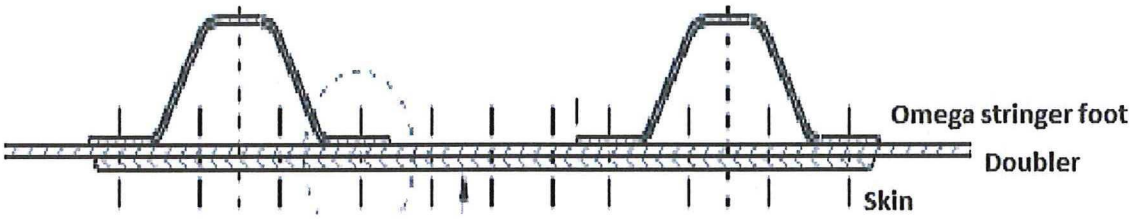

Figure 2.11: Bolted repair configuration with skin, stringer foot and doubler

stringer is introduced, namely an Omega-shaped stiffener. An example of a stiffened skin with Omega-stiffener and a doubler repair can be found in Figure 2.11.

These stiffeners also have a loading which can be transferred into the repair. This factor should also be taken into account during the justification of the repair.

2.4 Justification of a hybrid doubler repair

In the previous section it was discussed which are the extra elements which should be taken into account, now the next question is of course how the justification of such a hybrid repair can be performed. A repair should always be justified with a static and fatigue analysis. Within Airbus, different tools exist which can help to perform a justification of a repair. These tools were programmed in the past to handle purely metallic repairs on metallic fuselages. Hybrid repairs were not that common in use, and therefor could always be justified using some conservative assumptions or more time-consuming finite element investigations.

In the past, the fatigue justification of the repair was performed using an Airbus model where the skin was modelled with a bolted repair. The output of this model gives transferred forces and bore hole stresses, which are the stresses within the fastener holes. These bore hole stresses can then be used for the fatigue justification, since these hole bores are the fatigue-sensitive sites. Here, no stringer was modelled, since tests shown that the load transfer from the stringer to the doubler was negligible for metallic repairs on metallic fuselages with thermal loading. The justification had to be performed for the metallic skin and the metallic doubler.

Due to the changed configuration and the complex load transfer (due to the different materials, the anisotropic properties and the different stiffnesses) such assumptions cannot be made anymore. This leads to the need of a detailed analysis of how this load transfer can be modelled in a simple way. It is assumed that a load transfer takes place from the stiffener to the repair, which needs a new way of analysing the repair. Two ways are possible, namely:

- performing a finite element investigation for each hybrid repair.
- keeping the previous metallic justification process with applying some changes.

Performing a justification using a finite element model for each repair is too time consuming. Therefor the second option should be researched, namely the possibility to adapt the current Airbus model for hybrid repairs. This increases the simplicity and decreases the time needed to perform the analysis. Therefor, the different effects which were discussed in the previous section should be taken into account. This can be achieved by analyzing the effect of the stringer configuration on the load transfer and then by finding how this influences the different parameters of the repair.

The easiest way to model the extra load transfer is to find a factor which can be applied directly within the Airbus fatigue model, which will be called 'Load Increase Factor' or in short, LIF. This factor can then be applied on the different loading components which are applied within the Airbus fatigue model. Equation 2.4 shows an example for this factor applied on the longitudinal load component.

$$\sigma_{x_{adjusted}} = LIF \cdot \sigma_x \tag{2.4}$$

The goal of this research is to determine the load transfer between the stiffener and the repaired skin by using different models. The outcome should be a simplified, but accurate way of modelling the load transfer, preferably using an analytical equation. The different steps which will be taken in this research are described in Section 2.5.

Another assumption is that no composite fatigue will occur, and therefor only a fatigue justification of the doubler should be performed.

2.5 Research outline

As discussed in the previous sections, the goal of this thesis research is to define the load transfer between the original and the repaired fuselage structure. To find a solution, three problems need to be tackled, namely:

- the load transfer capability between the stiffened skin structure with the repaired structure.
- the effect of the thermal load on the load transfer capability.
- the determination of the best doubler thickness for the doubler.

The first step to find a solution is to perform a parametrical study with a finite element analysis using Abaqus. In this way the effect of the load transfer from the stiffened structure to the repair for different parameters such as the doubler thickness, fastener pitch and cut-out size can be determined. Using these models, also the thermal effect and the determination of the doubler thickness can be chosen.

The next step is to compare to see how the finite element is behaving with respect to the classical Airbus methods and tools. Using the Airbus internal stress tools, different models

are created and the behavior is compared. Using this, it can be seen how conservative these models are and so the best applicable model can be checked.

However, this research wants to go one step further, namely to skip the use of any tools to calculate the load transfer capability. This is possible by composing an analytical equation which takes into account all needed parameters and so the load increase can be easily calculated.

Chapter 3

Detailed Modelling of a Stiffened Repair

The use of finite element analysis (FEA) is these days widely spread in almost all branches in engineering. It is a computational technique which is used to obtain approximate solutions of boundary value problems. Aircraft are part of the most complex engineering problems, and thus FEA provides an ideal solution to solve problems, such as stress analysis, heat transfers and acoustics. To understand the full behavior of a hybrid doubler repair, a finite element model of this problem is created within Abaqus. This investigation is performed with a stiffened skin which has a cut-out for simulating the damage. A repair patch (doubler) is applied by mechanical fastening. The model will be used to determine the load transfer capability of the repair, the effect of the present stiffening elements and the thermal stresses acting on the doubler.

In Section 3.1 a general introduction and the basis of finite element analysis is given together with an overview of the most commonly used structural elements within FEA. Afterwards in Section 3.2, more details are given about the model, describing the used elements and the different parameters. Section 3.3 shows the results for the change of different parameters, such as the effect of different materials, temperature, doubler thickness, cut-out size, doubler size and loading. For all these parameters a finite element analysis is performed with different cases to research the effect of each parameter. The main conclusions of this study is given in Section 3.4. Figure 3.1 visualises the different steps taken in this chapter.

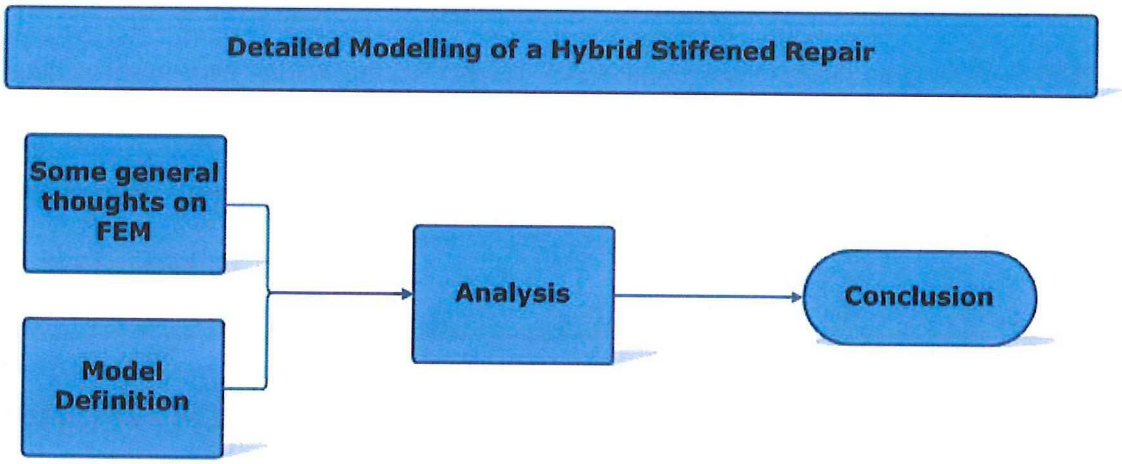

Figure 3.1: Flowchart of Chapter 3: Detailed Modelling of a Stiffened Repair

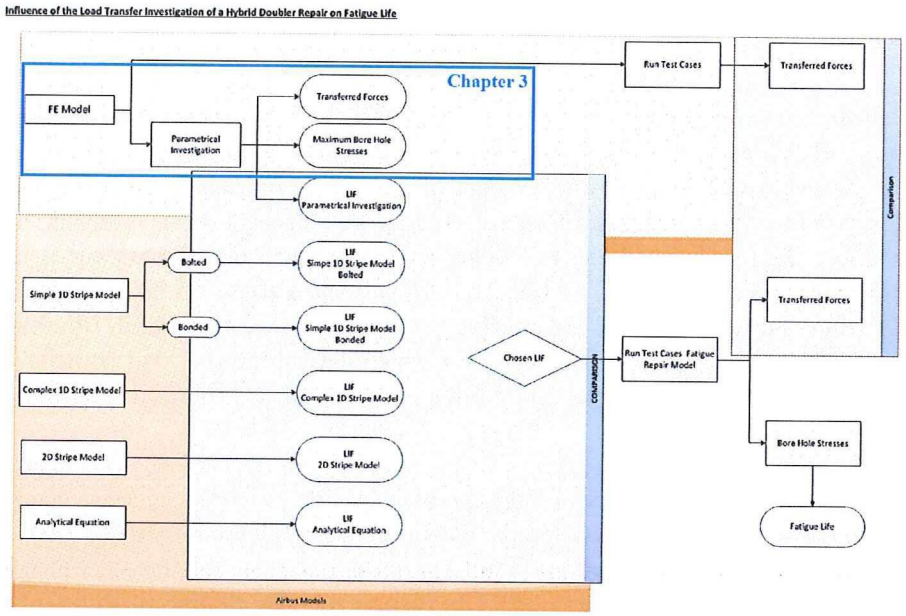

3.1 Some general thoughts on FEM

To research the load transfer capability of a hybrid repair, a detailed investigation was needed and done using a finite element analysis. The engineering software Abaqus was selected to perform the job, which combines a pre-processor, solver and post-processor in one program. However a finite element analysis can never be done blindly. Therefor this section will give a short overview of the main equations behind the models and an overview of the most commonly used structural FE models.

3.1.1 Main equations

Finite element analyses are used to solve boundary edge problems, which implies higher variational calculus. In this section, the main equations used will be shown. The main idea in FEA is the link between the stiffness matrix, the state vector (also known as the degrees of freedom) and the conjugate vector, which are linked via:

$$\mathbf{K}\delta = \mathrm{f} \tag{3.1}$$

where:

- **K** is the stiffness matrix

$$\left[K\right] = \begin{bmatrix} k_{11} & k_{12} & k_{13} & . & . & k_{1(n-1)} & k_{1n} \\ k_{21} & k_{22} & k_{23} & . & . & k_{2(n-1)} & k_{2n} \\ k_{31} & k_{32} & k_{33} & . & . & k_{3(n-1)} & k_{3n} \\ . & . & . & . & . & . & . \\ k_{(n-1)1} & k_{(n-1)2} & k_{(n-1)3} & . & . & k_{(n-1)(n-1)} & k_{(n-1)n} \\ k_{n1} & k_{n2} & k_{n3} & . & . & k_{n(n-1)} & k_{nn} \end{bmatrix} \tag{3.2}$$

- δ is the state vector, with some examples of the physical significance given in Table 3.1

$$\left[\delta\right] = \begin{bmatrix} u_1 & v_1 & u_2 & v_2 & . & . & u_{n-1} & v_{n-1} & u_n & v_n \end{bmatrix}^T \tag{3.3}$$

- **f** is the conjugate vector, with some examples of the physical significance given in Table 3.1

$$\left[f\right] = \begin{bmatrix} f_{u1} & f_{v1} & f_{u2} & f_{v2} & . & . & f_{u(n-1)} & f_{v(n-1)} & f_{un} & f_{vn} \end{bmatrix}^T \tag{3.4}$$

Table 3.1: Overview of the significance of u and f in different engineering problems [26]

Application Problem	State (DOF) vector u	Conjugate vector f
Structures & solid mechanics	Displacement	Mechanical Force
Heat conduction	Temperature	Heat flux
Acoustic Fluid	Displacement potential	Particle Velocity
General Flows	Velocity	Fluxes
Magnetostatics	Magnetic potential	Magnetic intensity

When the relation between forces is linear, but not homogeneous, Equation 3.1 generalises to:

$$\mathbf{K}\delta = \mathbf{f}_M + \mathbf{f}_I \tag{3.5}$$

where:

- $\mathbf{f}_I$ is the initial node force vector
- $\mathbf{f}_M$ is the vector of mechanical forces

From Table 3.1, it can be seen that for the hybrid doubler repair analyses both a structural as a heat conduction analysis is needed. A finite element problem is always solved using the steps as shown in Figure 3.2 and which are explained in detail in the next section.

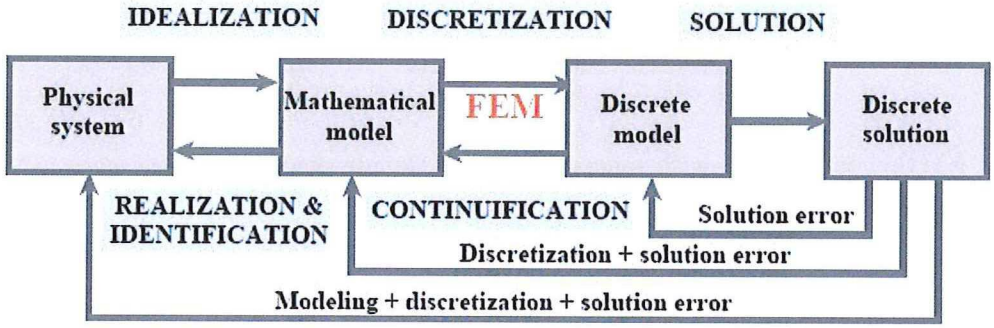

Figure 3.2: Simplified overview of the steps taken in a FEM approach [26]

3.1.2 Idealisation and discretisation of the problem

The first step is the *idealisation*, which means that the problem goes from a physical system to a mathematical model. In this step, the mathematical model is chosen which will be used to solve the problem. Main goal is to reduce the complexity of the engineering problem to be able to simulate the problem accordingly. This can be achieved by 'filtering' physical details that are not relevant to the design and analysis process. Since the analysis is done using the finite element program Abaqus, implicit modeling is used, meaning that the mathematical models behind the different element types are automatically generated during the mathematical idealisation.

The next step is the *discretisation* (or mathematical modeling) of the model, which is reducing the number of degrees of freedom (DOF) to a finite number. Using a finite element model, the mathematical model is disjointed in components of simple geometry, called finite elements, or also known as elements. The response of an element is then expressed in a finite number of degrees of freedom as the value of an unknown function at a set of nodal points. The response of our mathematical model is to be approximated by the repsonse of the discrete

model obtained by connecting or assembling the collection of all elements. All elements have an intrinsic dimensionality ranging from zero to three space dimensions (where in a dynamic anaylsis time can be another extra element), as shown in Figure 3.3. Each element posseses nodal points (nodes) which define the geometry of the elements and house the degrees of freedom (specifying the state of an element).

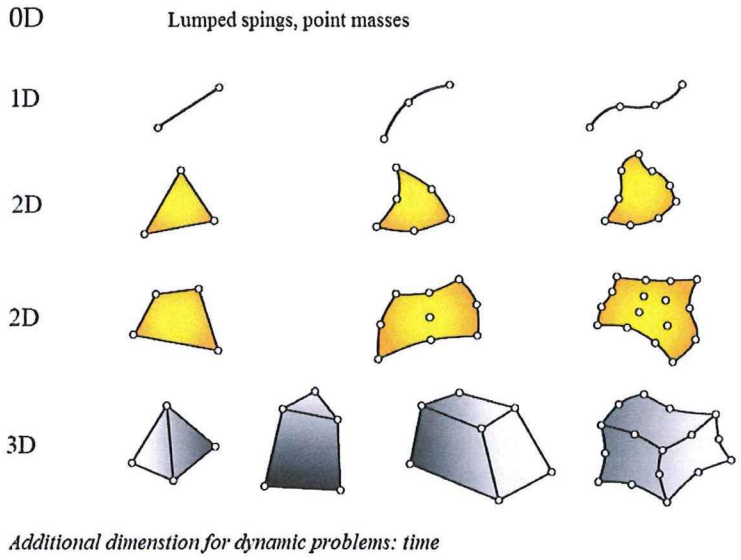

Figure 3.3: Overview of typical finite element geometries in different dimensions

3.1.3 Overview of the most common structural FEM-elements

There exist different classes of primitive strutural elements, see Figure 3.4. The main properties of each structural element are given below:

Bar A bar is a two-dimensional two-node element which can be loaded at both ends with only uni-axial forces in tension or compression. The structure has all axis of the bars lying in a common plane and the bars are connected in an ideal place joint, so no bending can be considered. The external forces can only act in the nodes and the lines of action of the forces are in the plane of the bars, leading to the fact that this element has only two degrees of freedom at each node, namely translation in x and y direction. [26]

Beam A beam is a two-dimensional two-node uni-axial element which has at both nodes three degrees of freedom (two displacements and a rotation), which makes it suitable for the modelling 2D-modeling of bent bars. Another beam-element which exists is a three-dimensional beam element, which also has two nodes, but in total six degrees of freedom, namely three displacements and three rotations, which makes it suitable for the modelling of three-dimensional bar structures. [26]

Tube/pipe A tube-element is two-node member which has in general six degrees of freedom at each node (three displacements and three rotations). The element can transmit moments, torques, forces and it can be loaded with internal pressure. [1]

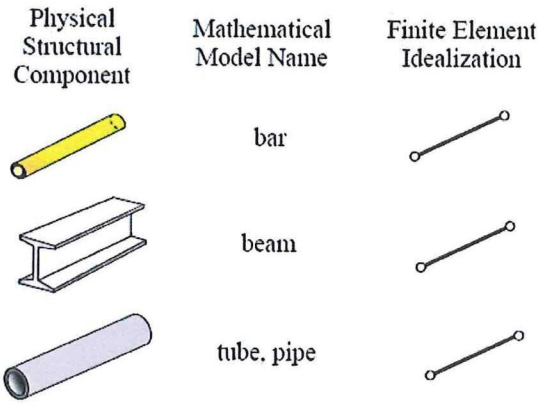

Figure 3.4: Overview of typical finite element geometries in different dimensions [26]

Another class of more complex finite elements are the continuum elements, which resemble structural components, viewed as contina. Two main elements are considered here, namely shell and solid elements, as can be seen in Figure 3.5.

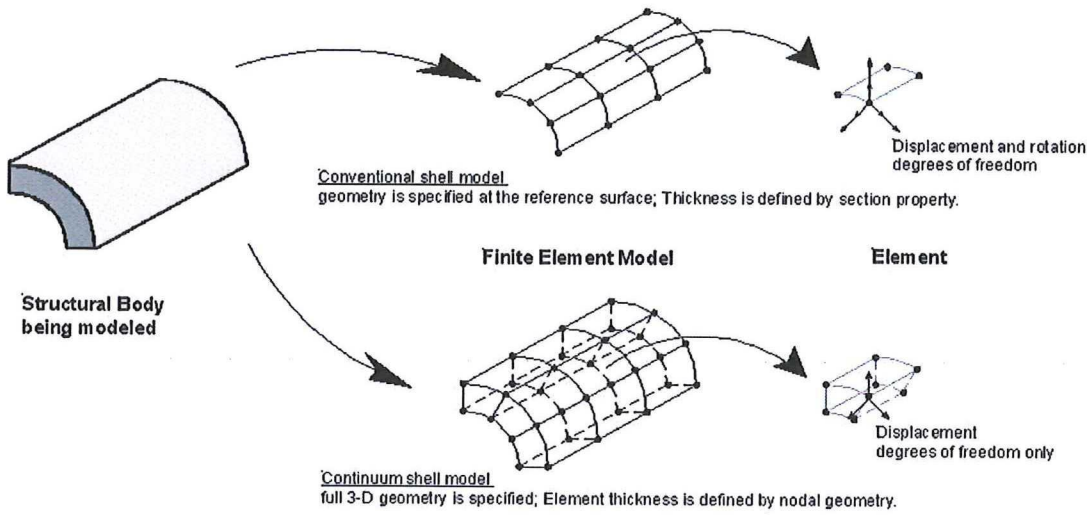

Figure 3.5: Overview of the two main types of continuum elements

Shell Elements A shell element is a combination of a plate element and a plane stress element, as can be seen in Figure 3.6. This leads to an element with in total five degrees of freedom per node, three DOFs from the plate element (one out-of-plane displacement and two rotations) and two DOFs from the plane stress element (two in-plane displacements).

From such a flat-shell element, a three dimensional solid finite element can be derived using degeneration of the shell elements. Due to this curvature, it is hard to connect precisely the surfaces of the shell model and the complexity only increases when multi-layered surfaces are used. However, a shell allows to create a mesh much easier with good quality elements.

Shell elements are used when the third dimensions is much smaller than the other two dimensions. Looking at the computational time, a shell model is stable and needs a relatively low computational time and disk space. Also the post-processing is faster than with a solid model. [1] [13]

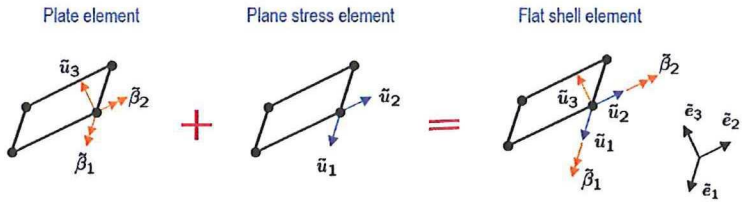

Figure 3.6: Example of a flat shell element

Continious shell element A continious shell element is also known as a solid element. The topology of this element is like a solid, but the solving equations are as for shell elements. These elements are three-dimensional stress/displacement elements for use in modeling structures that are generally slender, with a shell-like response but continuum element topology.

Using a solid model, the connections can be made much easier, decreasing the complexity of the problem. In a solid, tetrahedron elements are used, increasing the model complexity, however more realistic boundary conditions are possible for solids since faces are used instead of edges. Continious shell elements need more diskspace and have a longer runtime, which can jeopardise the use of large models. [1] [13]

3.2 Model Definition

The next step is to define the properties of the model. As described above, many different element types are possible, and the chosen types for this analysis are described in Section 3.2.1. Solving a finite element problem using software always generates many different data outcome sets. This implies that a selection must take place in which data will be used for the post-processing, which is explained in Section 3.2.2.

3.2.1 Properties of the model

The model is built-up from two types of general-purpose three-dimensional shell elements, named types S3 and S4R in Abaqus. These elements can be used both for thick as thin

shells, since the mathematical formulation of these elements converges to shear flexible theory for thick shells and classical theory for thin shells. Therefor it is possible to perform large strain analyses with these elements, since the shell formulation considers a finite-membrame strain. [1] [13]

The main type of element used is type S4R. It uses a reduced integration rule with only one integration point instead of four, making the calculation less computationally intensive. Therefor, the strain method also need to be modified so that one integration scheme plus hourglass stabilization can be obtained using an hourglass control parameter. This element type is used for all elements, except for the stiffeners. There, the other element is used, namely S3. It is obtained through the degeneration of the S4-element and so may exhibit overly stiff response in the membrane deformation.

Skin The skin is modelled as a shell element and represents nine skin bays and is limited by four stringers and four frames, as can be seen in Figure 3.7. It has a lay-up of 2/4/4/3.

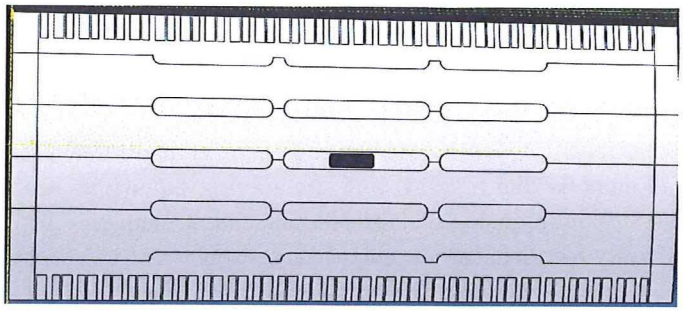

Figure 3.7: Overview of the modelled skin

Stringers The Omega-stringers are modeled as three-dimensional deformable shell elements, as can be seen in Figure 3.8. In this model, the stringer is extruded and the stringer feet is co-bonded to the skin. The stringer feet have a thickness of 1.4mm.

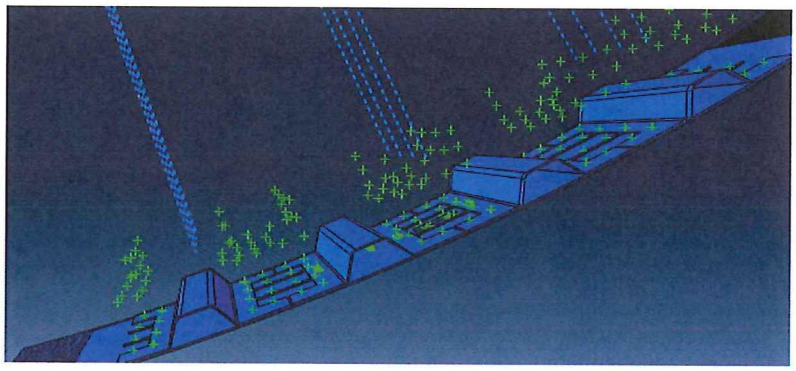

Figure 3.8: Overview of the stringers co-bonded to the skin

Cut-out The baseline cut-out has a size of 125 by 60mm and the corner radius is 12mm.

Doubler The baseline doubler has a size of 265 by 330mm and is made of Aluminium 2024-Clad with a thickness of 1.8mm, sized on iso-stiffness. On all sides of the repair, four rows of fasteners are placed between the cut-out edge and the doubler edge. The fastener pitch considered for this model is 19mm.

Loading The loading of the model simulates a representative loading for a skin bay on the side shell of the aft fuselage during the end of the cruise phase. The loading introduced on the model is:

- $\sigma_x = 63$MPa (longitudinal stress in the skin)
- $\sigma_y = 36.5$MPa (circumferential stress in the skin)
- $\tau_{xy} = 33$MPa (shear stress in the skin)
- $\sigma_{x-stringer} = 43.8$ MPa (longitudinal stress in the stringer)

As can be seen, the main loading direction is in-flight direction, but also the shear stress has a high component due to the location of the bay on the side shell.

Temperature The calculations are performed using an installation temperature of 23[$°C$], which corresponds to room temperature. The outside temperature of -15[$°C$] is assumed which is derived from the outside temperature for a mission flew on a standard day, under normal conditions, at the end of the cruise flight.

3.2.2 Outcome from the model

As already stated before, a finite element analysis generates lots of different data. However, not all data generated is useful to help solving the problem. Since the main interest is in the load transfer between the original stiffened structure and the repaired stiffened structure, post-processing is performed in three cases, namely:

- Maximal principle stress in the middle of the doubler (see Figure 3.9) which gives an idea of how much stress the repair is handling in the undisturbed stress field in the middle of the doubler.
- Transferred force at the corner fastener (see Figure 3.9), which show how much load is transferred from the stiffened co-bonded skin to the repair.
- Load Increase factor, which describes the amount of load which is transferred from the original structure to the repair, based on transferred forces.

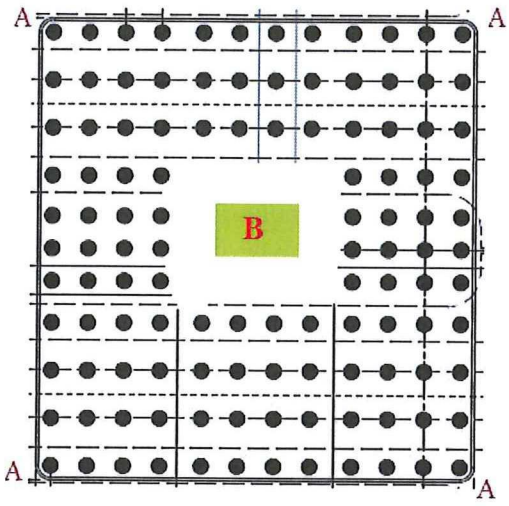

Figure 3.9: Overview of the locations where data for post-processing are exctracted

3.3 Analysis

In this section, the finite element investigation is described where different parameters are changed to see the effect on the load transfer capability of the repair. Following effects are researched:

- Effect of loading
- Effect of different material
- Effect of doubler thickness
- Effect of temperature
  - Installation temperature
  - Outside temperature
- Effect of cut-out size
- Effect of doubler size
  - Increasing the number of fastener rows
  - Increasing the fastener pitch

3.3.1 Effect of stringer load

The first effect which is researched is the influence of the loading. For this research, the loading within the skin will stay constant, but the load transferred by the stiffeners will change. An overview of the different stiffener loads which are analysed can be found in Table 3.2.

The analysis is performed for a doubler based on iso-stiffness. As can be seen from Figure 3.10, an increase of the stringer loading, leads to an increase of the transferred forces and the maximum principle stress in the middle of the doubler. This means that a load transfer takes place, meaning the stringer is de-loaded and extra load goes to the repair, even sized on iso-stiffness. The re-distribution can be explained due to the higher local bending due to the higher loads. This ratio of the change of this loading was defined as LIF and the values can be found in Table 3.2.

Table 3.2: Overview of the configurations analysed with different stringer loading

Configuration	Stringer Loading [MPa]	LIF
1	30.0	1.07
2	36.0	1.1
3	43.7	1.12
4	52.0	1.14
5	60.0	1.15

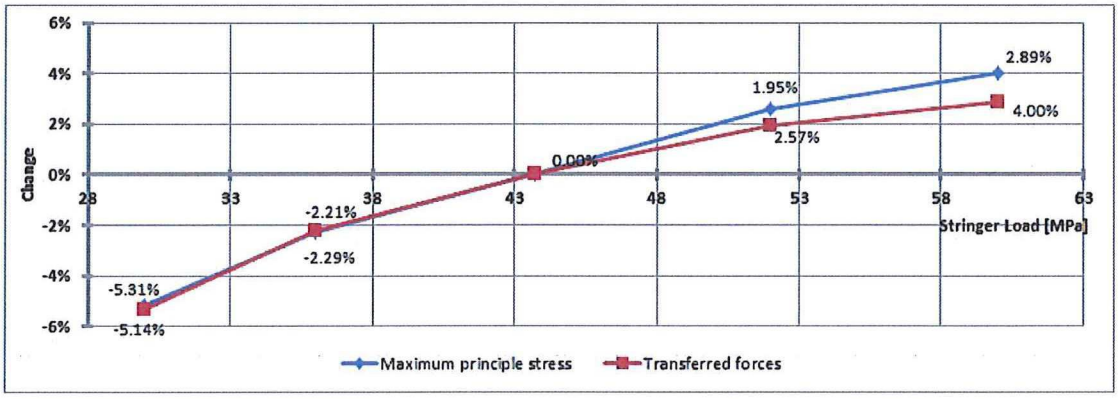

Figure 3.10: Change of maximum principle stress and transferred forces for different stringer loadings

3.3.2 Effect of different materials

A different material has different material properties, which leads to a different behaviour of the repair. In this study, four materials will be used which are realistic aircraft repair materials, namely:

- Aluminium, Al2024-Clad
- Titanium, Ti6Alv
- CFRP of a low-grade, with stacking 4/4/4/4
- CFRP of a mid-grade, with stacking 2/4/4/3

To be able to make a usable comparison between the materials, an iso-stiffness approach is used, as described in Section 2.3.2. Table 3.3 summarises the main properties of the materials. Due to the iso-stiffness approach, all repairs have a similar stiffness. This implies that the main parameter which can be researched now is the thermal expansion effect since all models are loaded with a temperature difference of $\Delta T = -38°C$. However only for the hybrid doubler repairs (metallic repair materials), the temperature effect is present. For the CFRP doublers, no thermal effect is expected since the thermal expansion coefficient of all materials is the same.

Table 3.3: Overview of the parameters used for comparing the effect of the use of different materials

	E-modulus [MPa]	**Thickness [mm]**	**Thermal Expansion Coefficient** $[/°C]$
Al2024-Clad	$65.5 \cdot 10^3$	1.8	$22 \cdot 10^{-6}$
Ti6Al4V	$110 \cdot 10^3$	1.2	$9.5 \cdot 10^{-6}$
CFRP 4/4/4/4	$57.3 \cdot 10^3$	2.0	$1.5 \cdot 10^{-7}$
CFRP 2/4/4/3	$50.5 \cdot 10^3$	2.4	$1.5 \cdot 10^{-7}$

The results are summarised in Figure 3.11. As can be seen, the CFRP 2/4/4/3-mid grade is set as basis for the comparison. This repair material leads to the lowest maximum principle stress and the lowest transferred forces. Comparing to CFRP 4/4/4/4-low grade shows that the results are almost identical and the differences are minimal. Both materials have the same thermal expansion coefficient as the original skin, so no thermal effect is considered here. However, CFRP 4/4/4/4-low grade is sized a little stiffer than the iso-stiffness criterion since it has a pre-defined stacking, and so thickness. As can be seen from this graph, a stiffer doubler leads to a load increase at the first fastener and at the middle of the doubler.

When these results are compared to Titanium, it can be seen that the stresses the load at the first fastener in the corner increases due to the thermal effect, which comes from the difference in thermal expansion coefficients between the original structure and the repair. It should be noted that also the considered Titanium doubler is a bit stiffer than iso-stiffness, since for Titanium 1.2mm is the minimum applicable thickness.

When the doubler is made of Aluminium, it can be seen that the difference with respect to the base case is the largest. Since the difference in thermal expansion coefficient between Alumiunium and CFRP is the largest, the thermal effect is the highest. This leads to an increase of the transferred force of 24.16% and an increase of 16% of the maximum principle stress in the middle of the doubler compared to the baseline case.

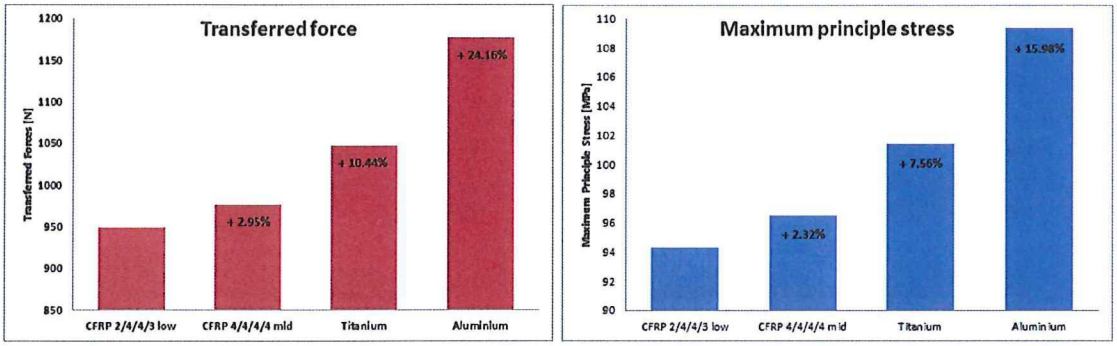

Figure 3.11: Change of maximum principle stress and transferred forces for different materials

Another interesting output which can be created is a visualisation of the transferred forces using vectors. Using vectors, it is possible to see both the direction as the magnitude of the transferred forces for all fasteners in the finite model.

From these figures (Figure 3.12 to 3.15, it can be seen that the direction of the vector for the different materials only change barely. However, the length (and thus magnitude) of the vector does change for the different materials.

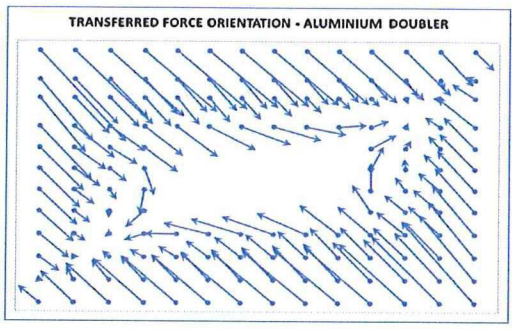

Figure 3.12: Vector visualisation of the transferred forces for an Aluminium doubler

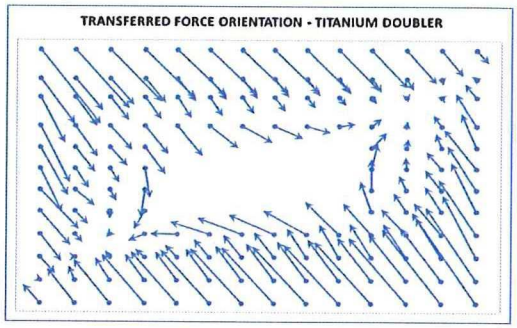

Figure 3.13: Vector visualisation of the transferred forces for a Titanium doubler

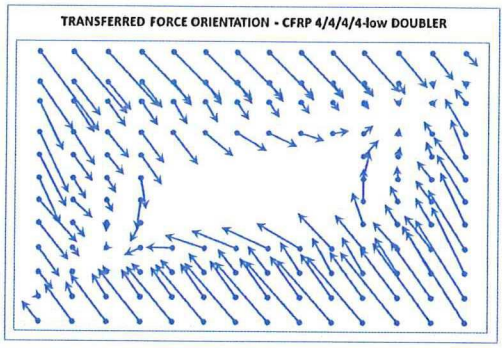

Figure 3.14: Vector visualisation of the transferred forces for a CFRP doubler with stacking 4/4/4/4 low-grade

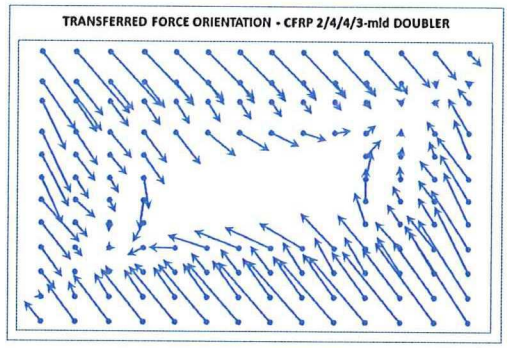

Figure 3.15: Vector visualisation of the transferred forces for a CFRP doubler with stacking 2/4/4/3 mid-grade

A third way of comparing the outcome of this study is using the Load Increase Factor, which shows how much the load is increased due to the stringer effect. The results are summarised in Table 3.4. As can be seen, both the Aluminium as the Titanium doubler have a similar Load Increase Factor (keeping in mind that the Titanium doubler is a bit stiffer). For both the composite doublers, almost no load exchange takes place.

Table 3.4: Load Increase Factor for the different materials (iso-stiffness)

Material	Thickness	LIF
Al2024-Clad	1.8	1.12
Ti6Al4V	1.2	1.13
CFRP 4/4/4/4	2.03	1.06
CFRP 2/4/4/3	2.4	1.05

3.3.3 Effect of doubler thickness

The second effect which is researched is the effect of the doubler thickness. Just as the effect of the material, the main parameter which is changed is the stiffness of the repair. Therefor, the results are splitted up in two subsections, one for each material. In this section, CFRP is not anymore analysed, since the focus of this thesis lies on hybrid doubler repairs. Also changing the thickness of a composite implies changing the number of plies, which results for almost every lay-up into a different stiffness.

Doubler Thickness Effect on Aluminium

The first material which will be researched with different doubler thicknesses is Aluminium. An overview of the different doubler thicknesses with their corresponding stiffness can be found in Table 3.5 where k is defined as

$$k = \frac{K_{repair}}{K_{original}} = \frac{E_{repair} \cdot t_{repair}}{E_{original} \cdot t_{original}} \tag{3.6}$$

Table 3.5: Overview of the different doubler thickness with their stiffness for an Aluminium Doubler Repair

Thickness [mm]	Stiffness [MPa]	k [-]
1.2	78 600	0.67
1.8	117 900	1
2.6	170 300	1.45
3.2	209 600	1.78

The effect of these different doubler thicknesses are plotted in Figure 3.16 for the maximum principle stress in the middle of the doubler and the transferred forces. As can be seen, two different effects on the Aluminium doubler thickness can be noticed, namely:

- A decrease of doubler thickness leads to higher stresses because of the decreased capacity of the repair to transfer the encountered stresses. This means that a thinner doubler is more critical when a doubler is sized on iso-stiffness in the main loading direction.
- A really thick doubler (a much higher stiffness than the original structure, here k=1.78) leads to higher loads and stresses, due to the load attraction of the surrounding structure.

This effect is supported when the Load Increase Factor is analyzed, see Table 3.6.

It can be concluded that the best solution for an Aluminium doubler repair is a doubler sized using:

$$t_{Aluminium} = \frac{1.05 \cdot E_{original} \cdot t_{original}}{E_{Aluminium}} \tag{3.7}$$

Table 3.6: Load Increase Factor for an Aluminium doubler with different thicknesses

Thickness	LIF
1.2	1.09
1.8	1.12
2.6	1.19
3.2	1.16

In practice, mostly this means taking the next available doubler thickness size available. Using this general rule for Aluminium, the doubler can carry all the load, without increasing locally the stiffness too much, through which load attraction is avoided.

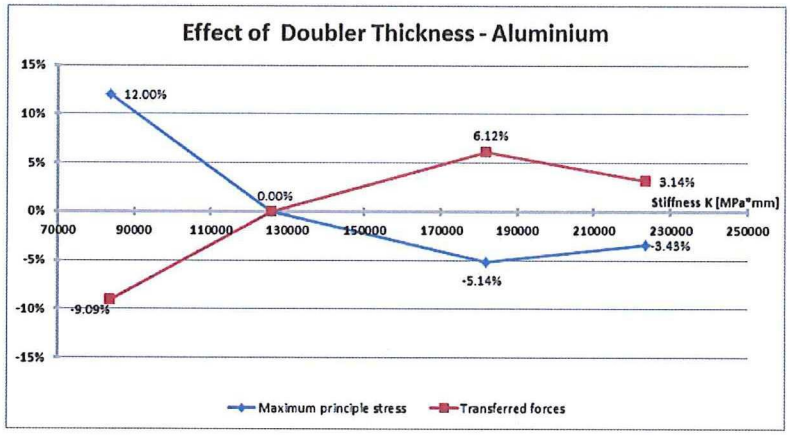

Figure 3.16: Change of maximum principle stress and transferred forces for different thicknesses for an Aluminium doubler

Doubler Thickness Effect on Titanium

For a Titanium doubler, the model has runned with the selected doubler thicknesses and accompanying stiffnesses as shown in Table 3.7. The results are summarised in Figure 3.17.

Table 3.7: Overview of the different doubler thickness with their stiffness for a Titanium Doubler Repair

Thickness t [mm]	Stiffness E [MPa]	k [-]
1.2	132 360	1.12
1.8	198 540	1.68
2.6	286 780	2.43
3.2	352 960	3

A similar behavior as for the Aluminium doubler can be found for the maximum principle stresses in the middle of the Titanium patch (see Figure 3.17 and Table 3.8). For the transferred forces, an increased stiffness of the repair leads to an increase of the transferred forces

at the corner fastener. This means that the load transfer capability of the Titanium doubler at the corner fastener is better than the Aluminium doubler load transfer capability. This can be explained due to the lower thermal effect which acts in the corner, leading to a better load transfer capability to the repair.

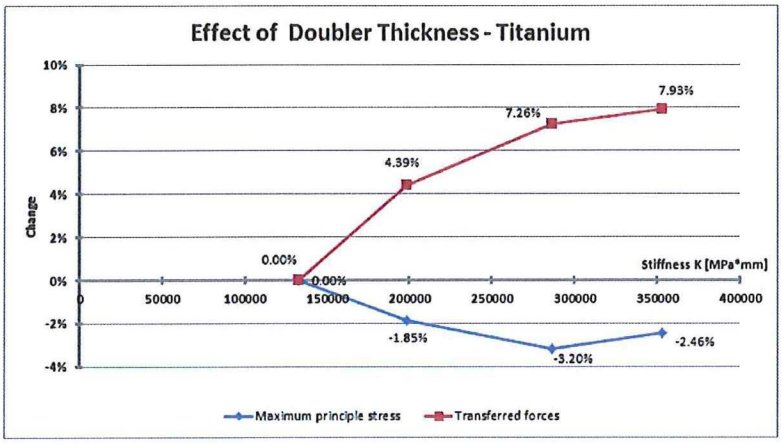

Figure 3.17: Change of maximum principle stress and transferred forces for different thicknesses for a Titanium doubler

Table 3.8: Load Increase Factor for a Titanium doubler with different thicknesses

Thickness	LIF
1.2	1.13
1.8	1.15
2.6	1.17
3.2	1.21

It can be concluded that for a Titanium doubler, even when the doubler is made three times stiffer than the original structure, the extra transferred force is only increased by 7.93%, compared to the case with the minimum doubler thickness possible for Titanium. This implies that no general sizing doubler rule is needed for Titanium, and that is best is just a doubler near the iso-stiffness criterion.

3.3.4 Effect of temperature

The additional thermal load can be of high importance to determine the extra thermal stress which is applied on the structure. This effect is researched in two different ways, namely the change of the external temperature and the change of the installation temperature. This effect is only researched for an Aluminium doubler repair, since it has the highest difference in thermal expansion coefficient with the original structure, as can be seen from Table 3.3. An overview of the different tested combinations is given in Table 3.9 for changing installation temperature and in Table 3.10 for changing outside temperature.

After running the models, it was seen that the temperature is modeled linearly. This means

Table 3.9: Overview of the different configuration studied for the temperature effect on the DFEM-model for different external temperatures

	Installation Temperature [°C]	Outside Temperature [°C]	Temperature Difference [°C]
Conf 1	$23°C$	$-15°C$	$-38°C$
Conf 2	$10°C$	$-15°C$	$-25°C$
Conf 3	$40°C$	$-15°C$	$-55°C$

Table 3.10: Overview of the different configuration studied for the temperature effect on the DFEM-model for different installation temperatures

	Installation Temperature [°C]	Outside Temperature [°C]	Temperature Difference [°C]
Conf 1	$23°C$	$-15°C$	$-38°C$
Conf 4	$23°C$	$-35°C$	$-58°C$
Conf 5	$23°C$	$23°C$	$0°C$
Conf 6	$23°C$	$70°C$	$47°C$

that for an equal temperature difference (ΔT), the same behavior is noticed for both the change of installation temperature as the change of outside temperature. Therefor, the results of all six different configurations can be gathered in the same plot, see Figure 3.18. From this plot, the linear dependence of the temperature is clearly seen. This is due to the fact that it is assumed that the thermal expansion coefficient of the material stays the same for each temperature. In reality, this is not the case.

As can be seen from Figure 3.18, the largest negative temperature difference leads to the highest thermal effect, both for the transferred force as for the maximum principle stress in the middle of the doubler. This implies that when the justification of the repair is performed with the highest theoretical temperature difference possible, the calculation will be too conservative. Therefor, it would be better to perform the calculations using the local temperature for the skin at the analysed bay. This effect is also seen when the Load Increase Factor is analysed, see Table 3.11.

Table 3.11: Load Increase Factor for a doubler with different thermal loadings

Temperature [°C]	LIF
47	1.04
0	1.06
-38	1.12
-58	1.24

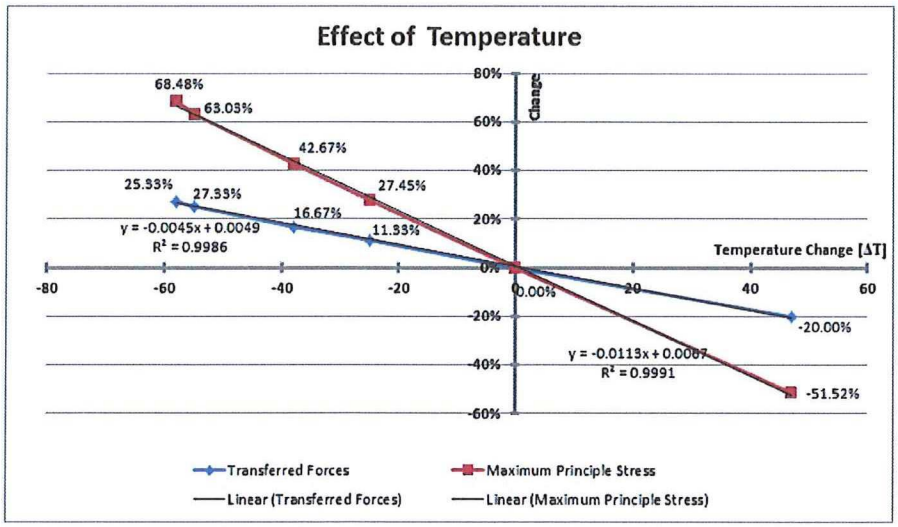

Figure 3.18: Change of maximum principle stress and transferred forces for different temperatures

3.3.5 Effect of cut-out size

The next effect is the cut-out size where three different cut-out sizes (representative for a SRM-repair(Structural Repair Manual)) are researched, namely

- 125 by 60mm, which is a nominal cut-out size.
- 200 by 200mm, a larger cut-out size.
- 300 by 300mm, an oversized cut-out size.

For this analysis, the applied doubler is made of Aluminium with a thickness of 1.8mm (sized based on iso-stiffness). When the size of the cut-out is increased, also the doubler size must increase, keeping the number of rows of fasteners between the cut-out and the edge of the doubler the same. The results are plotted in Figure 3.19.

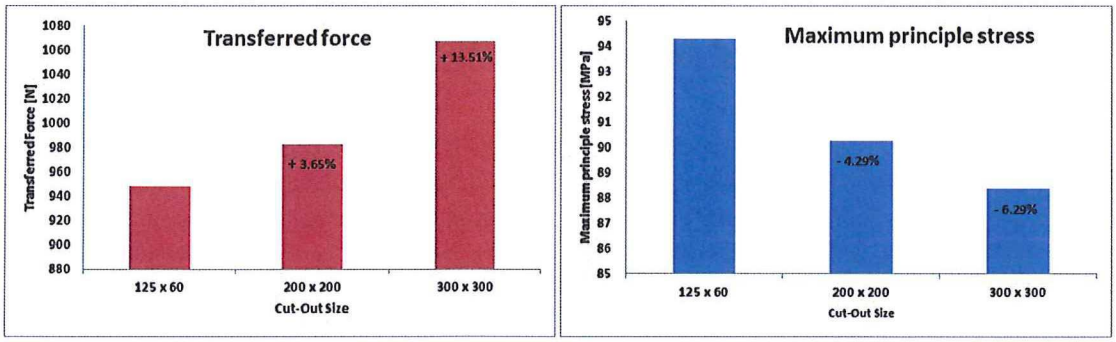

Figure 3.19: Change of maximum principle stress and transferred forces for different cut-out sizes

As can be seen, increasing the size of the cut-out has two main effects:

- an increase of the maximum principle stress in the middle of the doubler
- a decrease of the transferred force and an increase of the LIF

The increase of the maximum principle stress is explained due to the extra thermal stress which is introduced due to the larger doubler size. However due to the fastener force re-distribution (by adding extra rivet rows for the larger overlap area), the transferred force decreases taking up all extra force generated by the thermal effect. This effect should only be taken into consideration for a one-dimensional model, where the cut-out cannot be modelled. When a two-dimensional model is used (such as the Airbus fatigue model, see Appendix C), the fastener force re-distribution is already taken into account within the modelling, resulting in a different Load Increase Factor to be used, namely ($LIF_{adapted}$). The resulting values for the LIF can be found in Table 3.12.

Table 3.12: Load Increase Factor for a doubler with different cut-out sizes

Cut-out Size [mm]	LIF	$LIF_{adapted}$
125 x 60	1.12	1.12
200 x 200	1.15	1.14
300 x 300	1.18	1.15

3.3.6 Effect of the doubler size

The size of the doubler can be changed in two ways, namely by increasing the number of fastener rows around the cut-out or by increasing the fastener pitch between the fasteners. Both effects will be described in the following subsections.

Increasing the number of rivet rows

For this research, the number of rivet rows between the cut-out edge and the doubler edge is extended in longitudinal direction by adding two extra rows (also known as a 6 x 4 repair). The same is done for the circumferential direction (4 x 6 repair). The result for the transferred forces and the maximum principle stress in the middle of the doubler can be seen in Figure 3.20.

From this Figure, it can be seen that increasing the number of fastener rows is only slightly changing the maximum principle stress in the middle of the doubler. The maximum principle stress is changed slightly due to the increase of the thermal stress due to larger doubler size. The maximum transferred forces do change due to the same load re-distribution mechanism as was discussed in Section 3.3.5. Also here, this effect should not be considered for the determination of the Load Increase Factor. The difference for this factor is that this re-distribution is taken into account both by the one-dimensional as the two-dimensional Airbus models, and therefor always $LIF_{adapted}$ should be used . From Table 3.13 it can be seen that the Load Increase Factor only changes slightly.

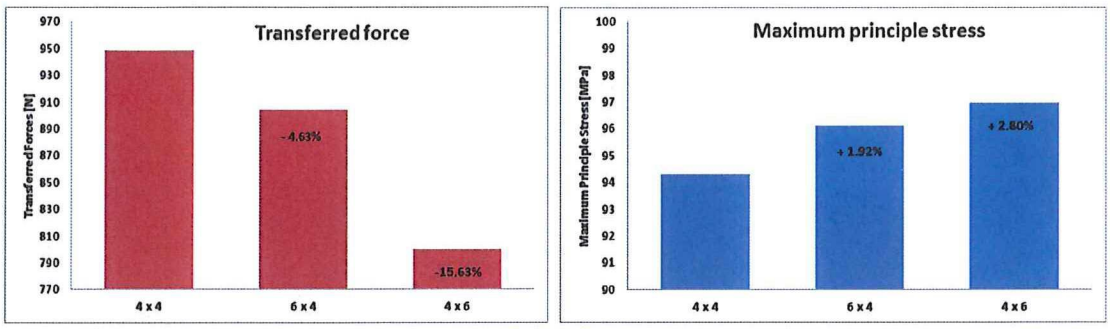

Figure 3.20: Maximum principle stress and transferred forces for different doubler sizes (increasing number of rivet rows)

Table 3.13: Load Increase Factor for a doubler with different numbers of fasteners around the cut-out

Fasteners around cut-out size	LIF	$LIF_{adapted}$
4 x 4	1.12	1.12
6 x 4	1.05	1.12
4 x 6	1.11	1.12

Increasing the fastener pitch

Another way of increasing the doubler size is by increasing the fastener pitch. When a repair is applied, the fastener pitch is mostly chosen in function of the local geometry. In this analysis, the fastener pitch is increased from 4D (≈19mm) to 6D (≈29mm), which are both representative fastener pitches for a skin doubler repair.

Increasing the fastener pitch leads to an increase of the doubler size, leading in this case to a relatively large increase of the transferred forces and a limited increase of the maximum principle stress, as can be seen from Figure 3.21. Increasing the fastener pitch increasing the bearing forces, which directly influences the transferred forces.

Another possibility is to increase the fastener pitch and keeping the same doubler size. This leads to a decrease of the number of fasteners which directly affects the load transfer, as discussed in [20].

The effect on the Load Increase Factor is described in Table 3.14. Also here a split-up is made between the LIF and the adjusted LIF ($LIF_{adapted}$) due to the re-distribution. Also here, when the load distribution is already taken into account within the simplified model, only a limited effect on the Load Increase Factor is found.

From this, it can be concluded that a repair can be better installed with a minimum fastener pitch. However, when the local geometry dictates an increase of the fastener pitch, then it is better to increase the doubler size, keeping the same number of rivets under the cut-out for a better load re-distribution.

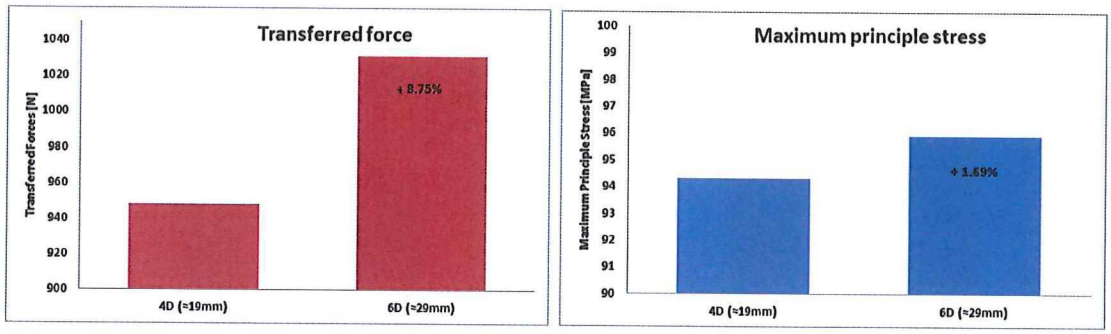

Figure 3.21: Change of maximum principle stress and transferred forces for different doubler sizes (increasing fastener pitch)

Table 3.14: Load Increase Factor for a doubler with changing fastener pitch

Fasteners pitch [mm]	LIF	$LIF_{adapted}$
4D ($\approx$ 19.2mm)	1.12	1.12
6D ($\approx$ 28.7mm)	1.17	1.13

3.4 Conclusion

After performing the finite element analysis, the first conclusions from this study can be made:

- It was seen in the different studies that the Load Increase Factor has only a main influence in the longitudinal direction. In circumferential direction, the influence of the Load Increase Factor is negligible (less than 1.5%).
- Increasing the **stringer load** results in an increase of the Load Increase Factor.
- The effect of the **material** showed that even for repair patches sized on iso-stiffness, large differences can occur in the load carrying capability of the model.
- From the **doubler thickness** effect, the different behavior of Aluminium for stiffer repairs should be kept in mind. Therefor it is advised to use as thicker repair thickness for Aluminium which is around 5% stiffer than the iso-stiffness sizing. For Titanium, a large increase of stiffness resulted in a relatively small influence on the load transfer capability of the model.
- The **temperature** showed the large influence of the thermal stresses on the behavior of the hybrid repair. The highest negative temperature difference had the largest effect on the load carrying capability of the model. Therefor the repair justification should be performed using a realistic value for the temperature of the skin at that bay, and not with a conservative temperature difference.

- Increasing the **size of the cut-out** leads to an increase of the maximum principle stress due to the increase of the thermal load of the enlarged doubler. The transferred decrease due to extra fasteners which are added and which cause a load re-distribution.

- The **doubler size** was increased in two ways. The increase of the number of rivet rows resulted in the same effects as were seen for enlarging the cut-out size. Increasing the fastener pitch leads to an increase of the transferred forces due to the higher bearing loads.

Chapter 4

Simplified Modelling of a Hybrid Repair using Airbus Models

Since it is impossible to justify every repair with a seperate detailed finite element investigation, industry designed some tools with simplifications which decrease the complexity of the model and the time needed to perform the calculation. Due to this, the tools are mostly more conservative. The goal of this chapter is thus to see how conservative these tools are for some configurations researched in the finite element investigation for a hybrid doubler repair configuration.

In Section 4.1, a short overview of the different available load transfer tools which are available within Airbus is given. Section 4.2 defines the selected configuration for comparison and selects the parameters which will be used. Also, here the idea behind the comparing of the models is given. Next section, Section 4.3, present and discusses the results of the different models. Section 4.4 gives the conclusion regarding the comparison and the applicability of the different models. A flowchart of these steps can be seen in Figure 4.1.

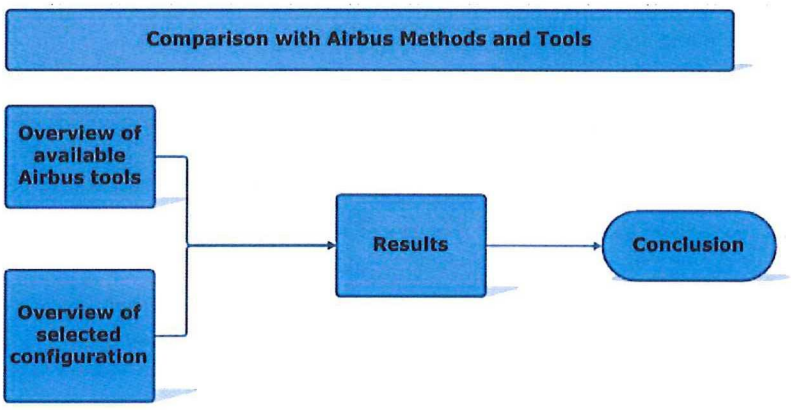

Figure 4.1: Flowchart of Chapter 4: Comparison with Airbus Methods and Tools

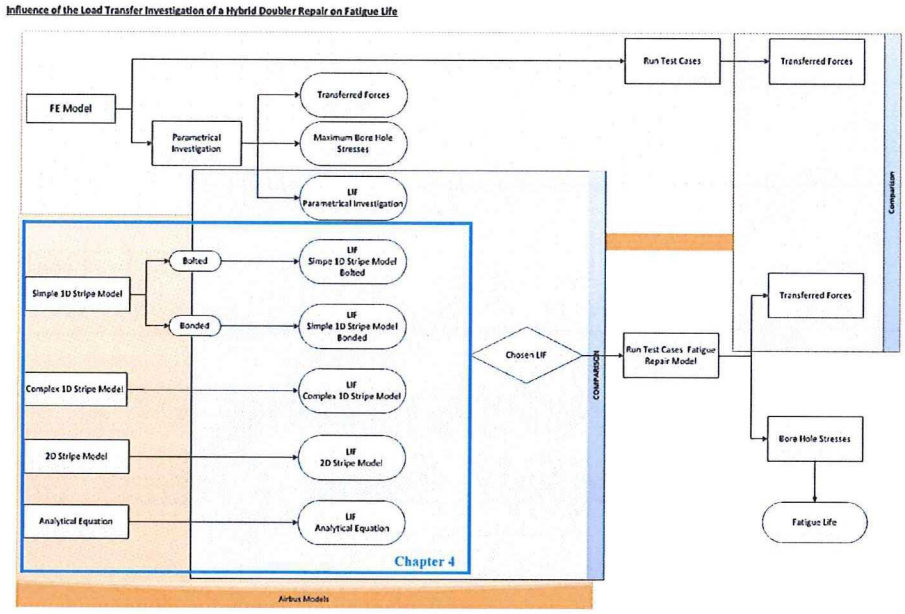

4.1 Overview of Airbus Tools

Within Airbus, different tools are available to analyse the load transfer within a structure. Most tools are based on simple and quick finite element models to give a good and realistic result of the load transfer. All Airbus internal tools are validated against test and can thus be used without question. This section will describe three different models which are used within Airbus, two based on one-dimensional stripe approaches, one on two-dimensional modelling and an analytical equations. Also the main limitations will be shortly described.

4.1.1 Simple stripe model

The first simplified one-dimensional stripe model is a finite element anaylsis based which idealises the actual joint by using beam elements for the plates and bush elements for the springs. The joint is defined by its number of plates and its number of fasteners. The plates are discretised by its material properties (Young's modulus, shear modulus and the thermal expansion coefficient) in the axis direction and its geometry, defined by width and thickness. This makes it possible to handle hybrid configurations. The loading and the boundary conditions are applied on the edges. The fluxes and bearing loads are extracted at each fastener and plate. Due to all these simplifications the computation time is very low.

Main limitation of the tool is that only linear behaviour can be modelled, thus no bending, nor shear load transfer. The model allows the introduction of a bonding line, leading to the ability of modelling easily a co-bonded stringer. A comparison will be made between:

- modelling the stringer co-bonded to the skin, which gives the best representation of the structure in reality and compared to the finite element model.
- modelling the stringer bolted to the skin, to study the conservatism of the modelling of the bondline.

4.1.2 Advanced stripe model

The second model is a more complicated, one-dimensional stripe model. This model is able to take into account the fastener flexibility and the secondary bending of the structure. It also based on a detailed finite element model where the fastener can be modelled in two ways, namely simplified and three-dimensional. In the case of three-dimensional modelling, the principle stresses are extracted where with a simplified fastener, only the transferred forces are extracted, as is the same for the repair model described in Appendix C. Using this model with three-dimensional fasteners, the fatigue law can be directly applied. Also here, the plates are discretised as described in the simple stripe model. The computation time is still low but is increased due to the more complex modelling of the three-dimensional fasteners and due to the out-of-plane effects.

One of the limitations of this model is that shear cannot be applied and that the loading needs to be uni-directional. Only bolted plates can be modelled, so no possibility to model a co-bonded structure. This can be solved in to ways, by:

- considering the skin and the stringer as one structure (integrated skin-stringer model).
- applying fasteners between the stringer skin to simulate the bonding.

It was chosen to use the second possibility to solve this problem, since this simulates better the different stiffnesses of the repair, skin and stringer. This also allows for a direct comparison with the calculation performed with the simplified stripe model.

4.1.3 Two-dimensional model

The third model is a two-dimensional detailed finite element model, in which several plates can be modelled, bolted or bonded. This model is loaded by fluxes and these can be applied in all directions: longitudinal, circumferential or shear flux. This model is more complex and needs more computational memory and time as the previous two models, though the results are more accurate. One of the main limitations of the model is that the fatigue life cannot be extracted directly.

4.1.4 Simplified analytical equation

Another way of analysing the load transfer which is used within Airbus is a simplified analytical equation which is linking the different stiffnesses and fluxes of a stiffened and un-stiffened repair.

The first parameter which plays a role into the load transfer is the stiffness. A ratio can be defined which represents the stiffness of the stiffened and unstiffened structure, see Equation 4.1.

$$K = \frac{\frac{K_{doubler}}{K_{doubler}+K_{skin}}}{\frac{K_{doubler}}{K_{doubler}+K_{skin}+K_{stringerfoot}}} \tag{4.1}$$

In this equation:

- K is the stiffness ratio between configuration with and without stringer foot
- $K_{component}$ is the stiffness of the different components

However, the stiffness is not the only effect playing a role in the load transfer capability. The next step is to introduce the loading into the equation, which is done using equation 4.2.

$$F = \frac{F_{stringerfoot}}{F_{nostringerfoot}} \tag{4.2}$$

Where:

$$F_{stringerfoot} = \frac{K_{doubler}}{K_{doubler} + K_{skin} + K_{stringerfoot}} \cdot (\sigma_{skin} \cdot t_{skin} + \sigma_{stringerfoot} \cdot t_{stringerfoot}) \tag{4.3}$$

$$F_{nostringerfoot} = \frac{K_{doubler}}{K_{doubler} + K_{skin}} \cdot (F_{skin} \cdot t_{skin}) \tag{4.4}$$

In these equations,

- F is the force flux for the different components
- K is the stiffness for the different components
- t is the thickness for the different components

The Load Increase Factor is then calculated using following formula:

$$LIF = K \cdot F \tag{4.5}$$

As can be seen, one of the main limitations of this formula is that the difference in thermal expansion coefficients is not taken into account. This implies that only a pure mechanical effect is taken into account in this approach.

4.2 Selected configuration for comparison

Now that the different models are introduced, it is time to set-up the model which will be used as base for the comparison. The same parameters as were discussed in the previous chapter will be handled. However, since a one-dimensional model need less input, a split-up is made between the inputs for the one-dimensional and two-dimensional models.

4.2.1 Inputs one-dimensional models

The relevant parameters for a one-dimensional model are summed below.

- **Location**
  The calculations are (as previously) performed for a representative skin side panel, at the aft side shell of the fuselage.

- **Material**
  The research is performed for Aluminium and Titanium.

- **Doubler Thicknesses**
  The base doubler thickness is again 1.8mm and three different doubler thicknesses are used for this comparison, namely 1.2, 2.6 and 3.2mm doubler thickness.

- **Temperature**
  The model is loaded with a thermal load of $-38°C$, which is related to the mid-range end-of-cruise standard-day mission. Also two other temperatures are used, namely when there is no temperature difference (pure mechanical effect) and the a thermal load of $-58°C$ which corresponds for a fuselage side panel to the lowest fatigue temperature which can be encountered.

- **Doubler size**
  The anaylsis will be performed for different doubler sizes namely by changing the number of rivet rows and the rivet pitch.

  - Increasing the number of rivet rows in longitudinal direction by adding two rows
  - Increasing the rivet pitch from 4D (four times the fastener diameter, ≈19.2mm) to 6D (≈ 28.7mm)

- **Loading**
  The models are loaded with fluxes which are linked to the stresses via:

$$F = \sigma \cdot t \tag{4.6}$$

  Where:

  - F is flux in $[\frac{N}{mm}]$
  - σ is the stress in $[MPa]$
  - t is the thickness in $[mm]$

For the one dimensional models, only the longitudinal load in the skin and the longitudinal component of the load in the stringer foot are taken into account, namely:

- $\sigma_x = 63\text{MPa}$
- $\sigma_{stringer} = 43.8\text{MPa}$

Also the **stringer load** will be changed to see the effect on the load transfer within the different models.

4.2.2 Inputs two-dimensional models

For the two-dimensional models, more inputs are needed. This section gives an overview to the additional parameters which are needed to perform the analysis.

- **Skin size** The skin is modelled with a size of 400 by 500mm.
- **Doubler size**
  The doubler has a size of 265 by 330mm. Alse here, the doubler size will be changed by changing the rivet pitch, as described above. Here two extra rivet rwos will not only be added in longitudinal direction, but also a case with thwo extra rivet rows in circumferential direction is researched.
- **Cut-out size**
  The baseline cut-out size has a dimension of 125 by 60mm. Two other cut-out sizes are researched with the two-dimensional model, namely 200 by 200mm and 300 by 300mm.
- **Loading**
  Also here the model is loaded with fluxes, but all loading components are taken into consideration. The circumferential and shear loading are:
  - $\sigma_y = 36.5\text{MPa}$
  - $\tau_{xy} = 33\text{MPa}$

4.2.3 Overview of all different configurations

A summary of all different configurations to be analysed is given in Figure 4.2

The post-processing of the outcome of the models is based on the procedure described in Appendix B. This means that the load transfer of the different models is extracted and compared to the values found in the finite element investigation.

		Material [-]	Stringer Loading [MPa]	Thickness [mm]	Temperature [°C]	Cut-out size x [mm]	Cut-out size y [mm]	Diameter [mm]	Number of rivet rows x [-]	Number of rivet rows y [-]	Pitch Long x [mm]
Baseline		Aluminium	43.8	1.8	-38	125	60	4.8	4	4	19.2
Stringer Loading	Conf.1	Aluminium	30	1.8	-38	125	60	4.8	4	4	19.2
	Conf.2	Aluminium	60	1.8	-38	125	60	4.8	4	4	19.2
Material	Conf.3	Titanium	43.8	1.2	-38	125	60	4.8	4	4	19.2
Doubler Thickness Aluminium	Conf.4	Aluminium	43.8	1.2	-38	125	60	4.8	4	4	19.2
	Conf.5	Aluminium	43.8	2.6	-38	125	60	4.8	4	4	19.2
	Conf.6	Aluminium	43.8	3.2	-38	125	60	4.8	4	4	19.2
Doubler Thickness Titanium	Conf.7	Titanium	43.8	1.8	-38	125	60	4.8	4	4	19.2
	Conf.8	Titanium	43.8	2.6	-38	125	60	4.8	4	4	19.2
	Conf.9	Titanium	43.8	3.2	-38	125	60	4.8	4	4	19.2
Temperature	Conf.10	Aluminium	43.8	1.8	0	125	60	4.8	4	4	19.2
	Conf.11	Aluminium	43.8	1.8	-58	125	60	4.8	4	4	19.2
Cut-out	Conf.12	Aluminium	43.8	1.8	-38	200	200	4.8	4	4	19.2
	Conf.13	Aluminium	43.8	1.8	-38	300	300	4.8	4	4	19.2
Rivet rows	Conf.14	Aluminium	43.8	1.8	-38	125	60	4.8	6	4	19.2
	Conf.15	Aluminium	43.8	1.8	-38	125	60	4.8	4	6	19.2
Pitch	Conf.16	Aluminium	43.8	1.8	-38	125	60	4.8	4	4	28.8
Pitch+Material	Conf.17	Aluminium	43.8	1.8	-38	125	60	4.8	4	4	28.8

Figure 4.2: Overview of configurations to be analysed using simplified Airbus tools

4.3 Results

The results are presented for each different parameter and a comparison is made between the different models and to the outcome of the finite element investigation.

4.3.1 Effect of stringer load

The first effect which is researched is the change of the stringer loading. This effect will be researched only for three configurations, namely a stringer load of 30, 43.7 and 60 MPa. The loading of the plate does not change. Figure 4.3 shows the change of the Load Increase Factor for those different stringer loadings.

		Stringer Loading [MPa]	Simple 1D Stripe bonded	Simple 1D Stripe bolted	2D Stripe Model	Complex 1D Stripe	Analytical	FEM
Baseline		43.8	1.23	1.15	1.11	1.39	1.88	1.12
Stringer Loading	Conf.1	30	1.19	1.13	1.09	1.31	1.72	1.07
	Conf.2	60	1.27	1.21	1.14	1.48	1.96	1.15

Figure 4.3: Load Increase Factors for different simplified Airbus models for a change of stringer loading

As can be seen, the behavior of the models is the same as was found for the finite element model. This means, the higher the loads which are transferred by the stringer, the higher the load transfer is to the repair (and all analyses are based on iso-stiffness). The results of the simple one-dimensional bolted stripe model and the two-dimensional model match the best with the load transfer found within the finite element investigation.

4.3.2 Effect of different materials

The second parameter which was researched was a change of material. In this study, only Aluminium and Titanium are selected to stay with the core of the research, namely hybrid doubler repairs. The results are summarised for a change of material in Figure 4.4.

		Material [-]	Simple 1D Stripe bolted	2D Stripe Model	Complex 1D Stripe	Analytical	FEM
Baseline		Aluminium	1.15	1.11	1.39	1.88	1.12
Material	Conf.3	Titanium	1.19	1.14	1.44	1.86	1.13

Figure 4.4: Load Increase Factors for different simplified Airbus models for a change of material

As can be seen, the two-dimensional stripe model leads to the lowest Load Increase Factor and gives a LIF which is almost identical to the one found using the finite element investigation. It can be seen that titanium leads to a higher load introduced in the skin, although the sizing is done one iso-stiffness criterion. However one exception can be seen, namely on the analytical equation where the Load Increase Factor increases. This means that not only the stiffness of the repair plays a role in the load transfer mechanism, but also other factors do have influence.

4.3.3 Effect of doubler thickness

Another parameter which is changed is the thickness of the doubler. This research is performed for two different doubler materials, namely Aluminium and Titanium. The results of the Load Increase Factors for the different models are described in Figure 4.5.

		Simple 1D Stripe bonded	Simple 1D Stripe bolted	2D Stripe Model	Complex 1D Stripe	Analytical	FEM
Baseline		1.23	1.15	1.11	1.39	1.88	1.12
Doubler Thickness Aluminium	Conf.4	1.14	1.13	1.12	1.34	1.97	1.09
	Conf.5	1.28	1.21	1.14	1.38	1.81	1.19
	Conf.6	1.33	1.27	1.18	1.36	1.77	1.16
Doubler Thickness Titanium	Conf.7	1.37	1.29	1.16	1.38	1.78	1.15
	Conf.8	1.46	1.35	1.19	1.34	1.73	1.17
	Conf.9	1.57	1.47	1.22	1.29	1.7	1.21

Figure 4.5: Load Increase Factors for different simplified Airbus models for a change of material thicknesses

The same behavior can be noticed for an Aluminium as for a Titanium doubler when the thickness is increased. For all models, an increase of the thickness leads to an increase of the Load Increase Factor. The two-dimensional stripe model shows the best match with the finite element investigation and the simple analytical equation shows an opposite behavior, due to the lack of the thermal effect within this model.

4.3.4 Effect of temperature

The next parameter is the effect of temperature. The behavior for the different Airbus internal tools can be found in Figure 4.6

		Temperature [°C]	Simple 1D Stripe bolted	2D Stripe Model	Complex 1D Stripe	Analytical	FEM
Baseline		-38	1.15	1.11	1.39	1.88	1.12
Temperature	Conf.10	0	1.08	1.05	1.11	1.88	1.06
	Conf.11	-58	1.21	1.16	1.55	1.88	1.24

Figure 4.6: Load Increase Factors for different simplified Airbus models for a change of temperature

When these number are plotted, see Figure 4.7, it can be seen that most models do behave linearly. The simple one-dimensional models and the two-dimensional model shows the best match with finite element solution. The complex one-dimensional stripe model leads to more conservative results. The analytical equation results in a constant LIF, since this parameter is not in a variable within the equation.

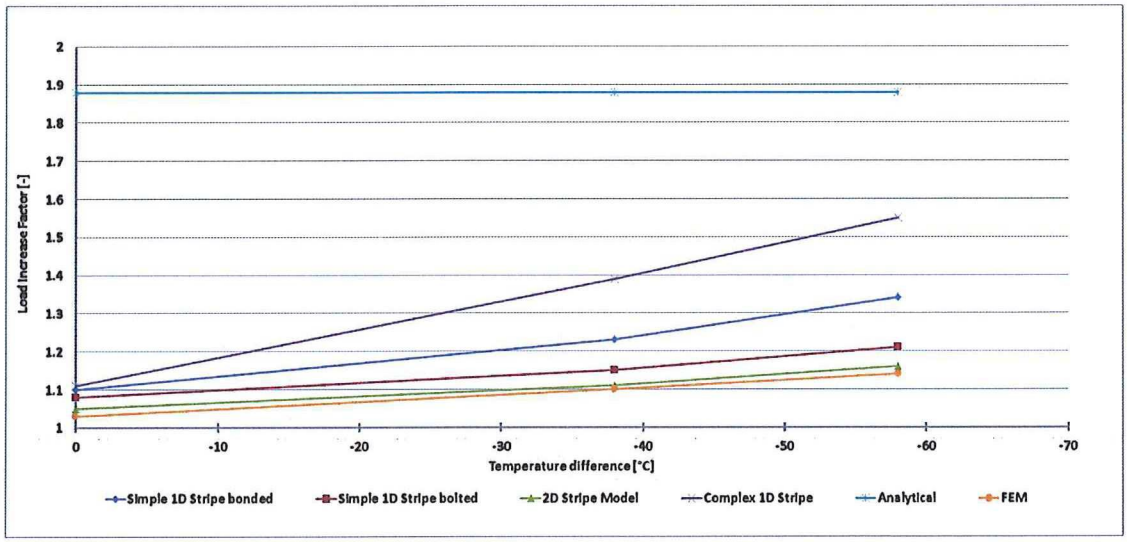

Figure 4.7: Load Increase Factors plotted for different simplified Airbus models for a change of temperature

4.3.5 Effect of cut-out size

Another influencing parameter which needs to be researched is the influence of the size of the cut-out. However, since it is assumed that the cut-out is not located under the stringer feet, no analysis can be performed for the one-dimensional models. The results can be found in Figure 4.8.

		Cut-out size x [mm]	Cut-out size y [mm]	Simple 1D Stripe bonded	Simple 1D Stripe bolted	2D Stripe Model	Complex 1D Stripe	Analytical	FEM
Baseline		125	60	1.23	1.15	1.11	1.39	1.88	1.12
Cut-out	Conf.12	200	200	-	-	1.08	-	1.88	1.15
	Conf.13	300	300	-	-	1.21	-	1.88	1.18

Figure 4.8: Load Increase Factors for different simplified Airbus models for a change of cut-out size

Increasing the cut-out size leads for the two-dimensional model to a small decrease of the Load Increase Factor. However, when the cut-out is made much larger, the Load Increase Factor increases dramastically. The same behavior was notified in the finite element model. For the analytical equation, the LIF does not change since the cut-out size is not a dependent parameter in this equation.

4.3.6 Effect of number of rivet rows

Another parameter of interest is the change of rivet rows next to the cut-out. Since the stripe models are only analyzed in one direction, an increase of number of fastener rows in y-direction can only be researched for the two-dimensional model. The results are summurised in Figure 4.9.

		Number of rivet rows x [-]	Number of rivet rows y [-]	Simple 1D Stripe bonded	Simple 1D Stripe bolted	2D Stripe Model	Complex 1D Stripe	Analytical	FEM
Baseline		4	4	1.23	1.15	1.11	1.39	1.88	1.12
Rivet rows	Conf.14	6	4	1.14	1.09	1.03	1.34	1.88	1.05
	Conf.15	4	6	-	-	1.11	-	1.88	1.11

Figure 4.9: Load Increase Factors for different simplified Airbus models for a change of number of rivet rows

When the number of rivet rows is increased in longitudinal direction, the Load Increase Factor decreases for all models, which loeads to the same behavior as was seen in the finite element stuyd. This is due to the fact that an iincrease of the number of rivet rows leads to more rivets over which the load can be distributed.

When the number of rivet rows is increased in the y-direction, the two-dimensional model shows no difference in Load Increase Factor, just as saw in the finite element modelling.

Once again, the analytical equation leads to a much higher and constant Load Increase Factor, due tot he fact that also the number of rivets is not an influencable parameter in this equation.

4.3.7 Effect of fastener pitch

The last parameter which is researched is the influence of the fastener pitch. Here, four configurations are tested, minimum and maximum fastener pitch for two materials (Aluminium and Titanium). The results can be found in Figure 4.10.

		Pitch Long x [mm]	Simple 1D Stripe bonded	Simple 1D Stripe bolted	2D Stripe Model	Complex 1D Stripe	Analytical	FEM
Baseline		19.2	1.23	1.15	1.11	1.39	1.88	1.12
Pitch	Conf.16	28.8	1.28	1.24	1.18	1.44	1.88	1.17
Material	Conf.1	19.2	1.27	1.19	1.13	1.44	1.86	1.12
Pitch + Material	Conf.17	28.8	1.34	1.26	1.22	1.51	1.86	1.16

Figure 4.10: Load Increase Factors for different simplified Airbus models for a change of rivet pitch

As can be seen, for both materials, an increase of the fastener pitch leads to an increase of the LIF. However the increase of the Load Increase Factor is much larger in the Airbus models than was seen in the finite element investigation. The analytical equation leads to a high and constant Load Increase Factor, since also this parameter is no part of the equation.

4.4 Conclusion

It can be concluded that all models (except the analytical equation) can be used to perform the load transfer analysis. When compared to the finite element solution, it is found that the two-dimensional model leads to the best match regarding the Load Increase Factor. The other models (simple one-dimensioonal stripe models bolted and bonded & and complex one-dimensional stripe model) lead to higher more conservative results. The analytical equation which only based on fluxes and stiffness ratio shows a bad match with all other models. An overview of all LIFs for all configurations is given in Figure 4.11.

		Simple 1D Stripe bonded	Simple 1D Stripe bolted	2D Stripe Model	Complex 1D Stripe	Analytical	FEM
Baseline		1.23	1.15	1.11	1.39	1.88	1.12
Stringer Loading	Conf.1	1.19	1.13	1.09	1.31	1.72	1.07
	Conf.2	1.27	1.21	1.14	1.48	1.96	1.15
Material	Conf.3	1.27	1.19	1.14	1.44	1.86	1.13
Doubler Thickness Aluminium	Conf.4	1.14	1.13	1.12	1.34	1.97	1.09
	Conf.5	1.28	1.21	1.14	1.38	1.81	1.19
	Conf.6	1.33	1.27	1.18	1.36	1.77	1.16
Doubler Thickness Titanium	Conf.7	1.37	1.29	1.16	1.38	1.78	1.15
	Conf.8	1.46	1.35	1.19	1.34	1.73	1.17
	Conf.9	1.57	1.47	1.22	1.29	1.7	1.21
Temperature	Conf.10	1.1	1.08	1.05	1.11	1.88	1.06
	Conf.11	1.34	1.21	1.16	1.55	1.88	1.24
Cut-out	Conf.12	-	-	1.08	-	1.88	1.15
	Conf.13	-	-	1.21	-	1.88	1.18
Rivet rows	Conf.14	1.14	1.09	1.03	1.34	1.88	1.05
	Conf.15	-	-	1.11	-	1.88	1.11
Pitch	Conf.16	1.28	1.24	1.18	1.44	1.88	1.17
Pitch + Material	Conf.17	1.34	1.26	1.22	1.51	1.86	1.16

Figure 4.11: Overview of Load Increase Factors of all analysed configurations

Chapter 5

Analytical Equation for the Load Transfer

As was shown in the previous chapters, it is hard and time-consuming to make a detailed estimation of the load transfer. Different tools are available, ranging from simple stripe models to the more complex finite element models. In these models, different parameters need to be taken into account, such as the different stiffnesses, the number of rivets in each direction, the load carried by the stiffeners and so on. It was shown that the simplified models cannot handle all these parameters and the more complex ones are able to handle all parameters, but need therefor more set-up time and computational power.

This last chapter will try to present an alternative analytical equation based on the finite element investigation that can describe the load transfer of the repair. The equation is based on the results which were found in the finite element study and which were already compared to the Airbus internal outcomes. In Section 5.1 the new analytical equation is step-wise presented and the used parameters are described. This equation provides a Load Increase Factor, which can be applied directly in the Airbus fatigue model (which is a model where no stringer foot can be modelled) or any simplified one-dimensional Airbus model. Then this equation has been tested for three different configurations in Section 5.2 with the Airbus repair model. Here, the calculated Load Increase Factor is applied on the fatigue repair model and the result is compared to the outcome of the finite element model. The last section, Section 5.3, provides a conclusion regarding the mathcing of the solutions. These steps are visualised in a flowchart, see Figure 5.1.

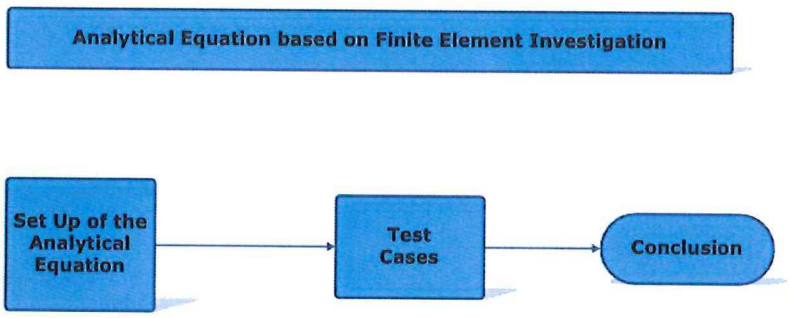

Figure 5.1: Flowchart of Chapter 5: Analytical Equation for the Load Transfer

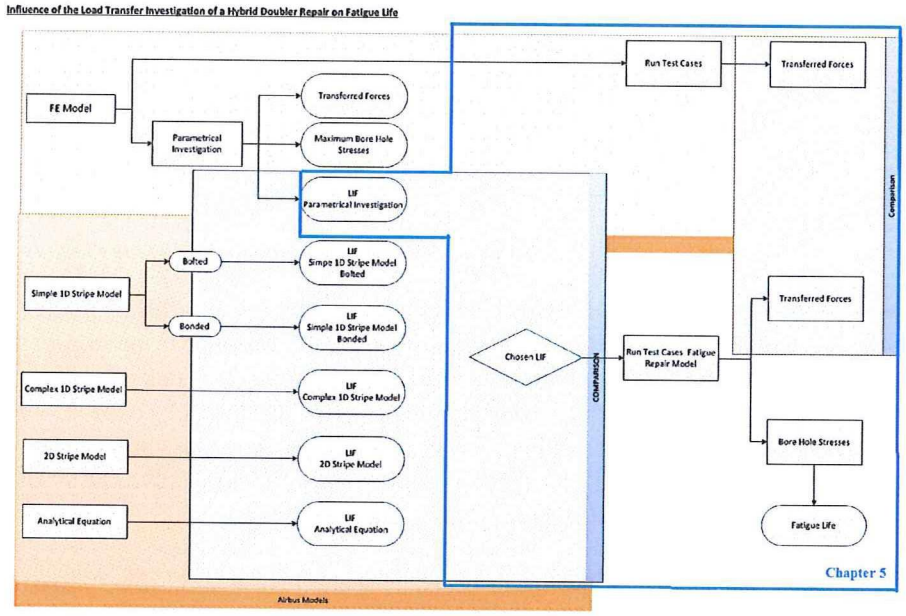

5.1 Set-Up of Analytical Equation for the Load Transfer

As was seen in Chapter 2, the internal Airbus model for calculating the fatigue life of a doubler repair cannot model any stringers. In the past, this could be easily handled, due to the fact that the same material was used and tests showed that the load transfer from stringer to the repair was limited. However, when a hybrid doubler repair is considered, the load transfer of the stringer to the repair cannot longer be ignored. Therefor a fast and straightforward solution had to be found to determine the load transfer from the doubler repair. Since no test data are available, a parametric finite element investigation was performed. Based on this outcome, it was possible to create an analytical equation which gives the load transfer for a certain configuration. This section describes the different elements in this equation.

5.1.1 Effect of stringer load

The first effect which is considered is the change of the stringer loading. This effect is considered the main effect acting on the load transfer, and therefor it can be estimated using Equation 5.1. This equation is derived from the plot obtained with the finite element analysis, see Figure 5.2

$$LIF = 2 \cdot 10^{-6}\sigma^3_{stringer} - 0.0003 \cdot \sigma^2_{stringer} + 0.0184 \cdot \sigma_{stringer} + 0.737 \tag{5.1}$$

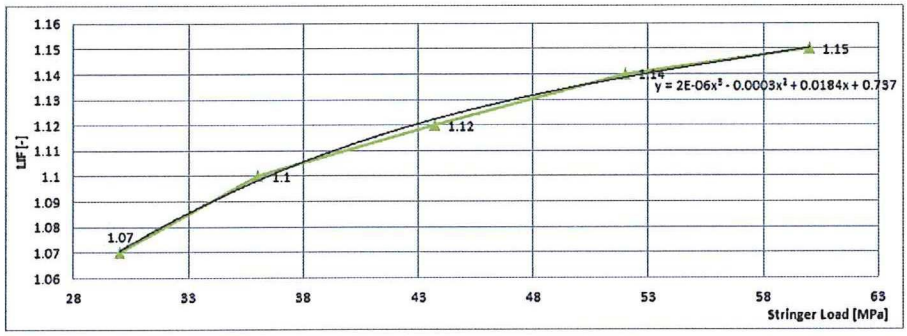

Figure 5.2: Load Increase Factor versus the stringer loading for an Aluminium doubler

5.1.2 Effect of thickness

The second effect is the influence of the doubler thickness. This parameter has a direct influence on the stiffness of the repair. In the finite element method, a different behavior was noticed for Aluminium as for Titanium, therefor the two materials are seperatly considered, each with its own correction factor.

Aluminium For Aluminium, a polynomial behavior is obtained, as can be seen in Figure 5.3 when plotting the Load Increase Factor versus the stiffness (between the original structure and the repair).

This leads to following relation:

$$LIF_t = -0.1041 \cdot K^3 + 0.1504 \cdot K^2 + 0.2391 \cdot K + 0.7146 \tag{5.2}$$

Titanium For Titanium, a different behavior was obtained, namely an increase of the stiffness ratio always resulted in an increase of the Load Increase Factor, as can be seen from Figure 5.4. It implies that even when a repair is sized based on iso-stiffness, a different behavior is found. This can be explained by a difference in the location of the neutral line, as illustrated in Figure 5.5. Changing the thickness of the material, will change the position of the neutral line, leading to a different bending behavio

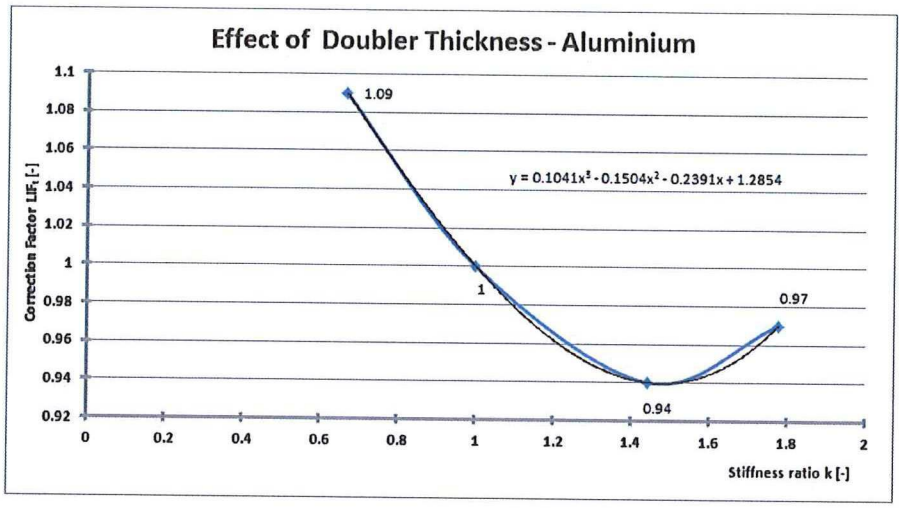

Figure 5.3: Increase of the Load Increase Factor versus the stiffness ratio for an Aluminium doubler

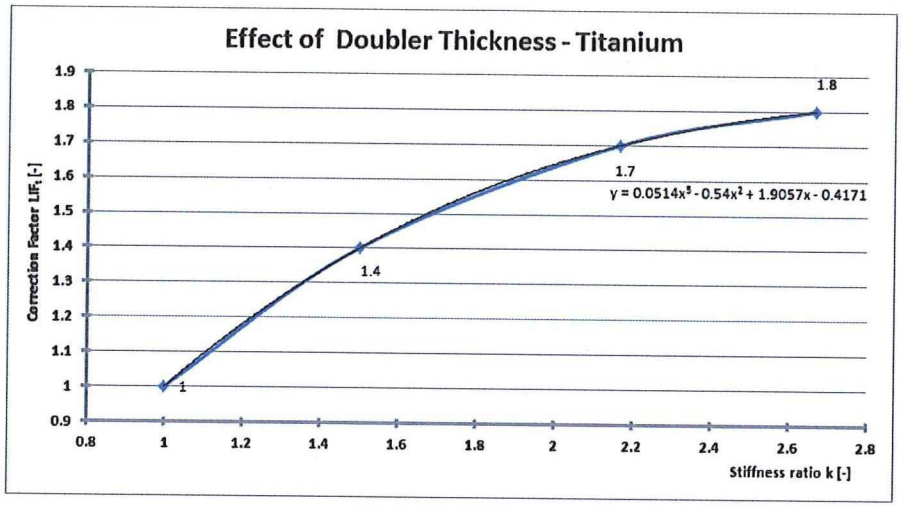

Figure 5.4: Load Increase Factor versus the stiffness ratio for a Titanium doubler

For Titanium, this leads to following relation:

$$LIF_t = 0.0514 \cdot K^3 - 0.54 \cdot K^2 + 1.9057 \cdot K - 0.4171 \tag{5.3}$$

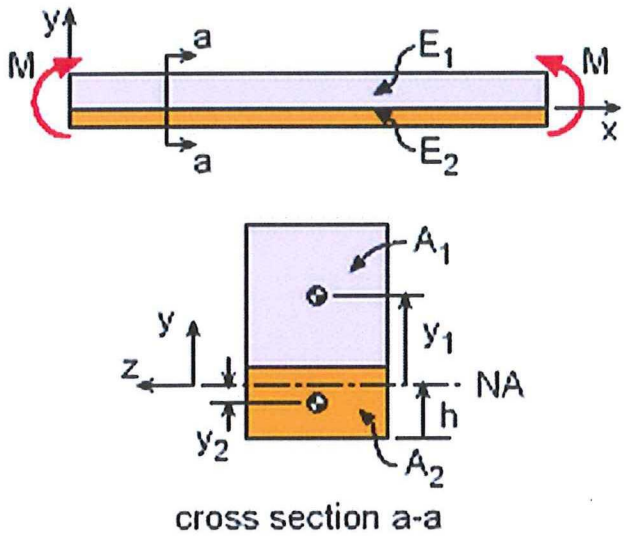

Figure 5.5: Location of the neutral axis for a hybrid configuration [8]

5.1.3 Effect of temperature

The third effect which had to be included is the effect of temperature. In the different studies which were performed it was observed that the temperature effect only plays a role when there is a large difference between the thermal expansion coefficients of the materials.

Aluminium doubler In the finite element investigation it was shown that this effect can be modelled linearly (see Figure 5.6). Due to this linearity for Aluminium, this factor can also be applied as a factor on the LIF, given by Equation 5.4:

$$LIF_T = -0.0045\Delta T + 1.0044 \tag{5.4}$$

Titanium doubler Since the difference of the thermal expansion coefficients between a Titanium doubler and a CFRP skin is rather small, it is assumed that the thermal effect is negligible.

5.1.4 Effect of cut-out

The next effect which is considered is the size of the cut-out. As was seen in the finite element investigation, an increase of the cut-out size lead to a load re-distribution. There for a split-up need to be made between one-dimensional and two-dimensional Airbus models, since this effect is already taken into account within a two-dimensional Airbus model. For the one-dimensional case, the Load Increase Factor is described by Equation 5.5.

$$LIF_{cut-out} = \frac{L_{cut-out} - 125}{30} \cdot 0.01 + 1 \tag{5.5}$$

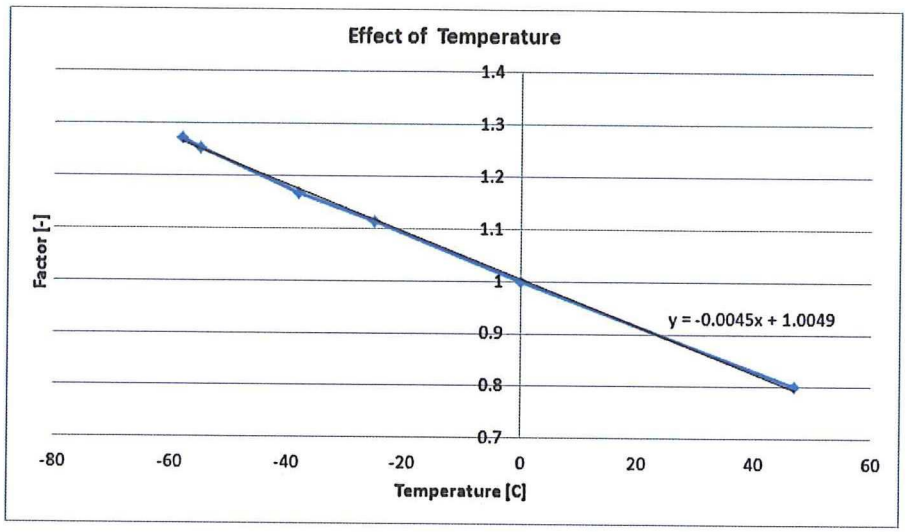

Figure 5.6: Increase of the Load Increase Factor versus the temperature for an Aluminium doubler

When a two-dimensional model is used, the Load Increase Factor is described by Equation 5.6.

$$LIF_{cut-out} = \frac{L_{cut-out} - 125}{50} \cdot 0.01 + 1 \tag{5.6}$$

For any cut-out smaller than 125mm, no extra factor need to be taken into account for both models and therefor $LIF_{cut-out} = 1$.

5.1.5 Effect of number of rivet rows

As was seen in the finite element investigation, a load re-distribution takes place when extra rivet rows are added. However, this load re-distribution effect, is already taken into account, so when purely the load transfer is taken, it was seen that no extra load transfer was found, recall Table 3.13. Thus this factor equals one.

5.1.6 Effect of the fastener pitch

Also for this parameter, a split-up was made between the load re-distribution and the load transfer, see Table 3.14. It was found that increasing the rivet pitch only slightly changes the load transfer. Therefore also this parameter equals one.

5.1.7 Combination of all parameters

All parameters described above can be combined into one equation, namely:

$$LIF = \left(2 \cdot 10^{-6} \cdot \sigma^3_{stringer} - 0.0003 \cdot \sigma^2_{stringer} + 0.0184 \cdot \sigma_{stringer} + 0.737\right) \cdot LIF_t \cdot LIF_T \cdot LIF_{rivetrows} \cdot LIF_{rivetpitch} \tag{5.7}$$

Where:

- LIF_t is the factor for compensating the thickness, given by Equation 5.2 for Aluminium and Equation 5.3 for Titanium.
- LIF_T is the factor for compensating the temperature effect for Aluminium and given by Equation 5.4, for other materials $LIF_T = 1$.
- $LIF_{cut-out}$ is the factor for compensating the cut-out size effect and is defined by Equation 5.5.
- $LIF_{rivetrows}$ is the factor for compensating the amount of rivet rows and equals 1.
- $LIF_{rivetpitch}$ is the factor for compensating the change in rivet pitch and equals 1.

All these equations are also combined in an Excel-template, so that a fast change of parameters is possible, see Figure 5.7

Stringer			
Stringer Load	σstringer	[MPa]	45

Doubler			
Material		[-]	Aluminium
Young's Modulus	E	[MPa]	65500
Thickness	t	[mm]	1.8

Skin			
Young's Modulus	E	[MPa]	65500
Thickness	t	[mm]	1.8

General			
Temperature difference	ΔT	[]	-38
Cut-out length	Lcut-out	[mm]	130
Number of Rivet rows		[-]	4
Rivet pitch	D	[mm]	4

LIF	1.14

Figure 5.7: Printscreen of the Excel-sheet created for the automatic LIF calculation

5.2 Test cases

After defining the general equation, it is tested for different cases. For each case, the Load Increase Factor is calculated using the analytical equation and this outcome is then loaded into the repair model. The same configuration is modelled using the finite element model, where the skin and stringers can be seperatley loaded. The outcomes will be compared based on transferred forces. From the Airbus fatigue model, also the bore hole stresses can be determined, via which the fatigue life for the doubler is calculated.

5.2.1 Test case 1 - Pure mechanical loading

The first case which will be analysed is a pure mechanical load case, so without any thermal effect. The model has an isotropic composite skin and the applied doubler is sized on iso-stiffness. The model uses following inputs, as defined in Table 5.1. The LIF is calculated using Equation 5.7 and equals 1.10 which is applied in the fatigue model as described in Appendix C.

Table 5.1: Overview of the inputs used for test case 1

Parameter	Unit	Value
Cut-Out Size	[mm]	100 x 100
Doubler Size	[mm]	283.6 x 270.85
Skin Size	[mm]	425 x 406
Fastener Pitch	[mm]	4D (≈19.2mm)
Doubler Thickness	[mm]	1.8
Doubler Stiffness	[MPa]	65500
Skin Lay-Up	[-]	4/4/4/4 (≈2.0mm)
Skin Stiffness	[MPa]	57593.1
Skin Loading σ_x / σ_y / τ_{xy}	[MPa]	60 / 40 / 20
Stringer Loading	[MPa]	30
Temperature Loading	[°C]	0

Running this case using the finite element model and the Airbus fatigue model leads to the outputs shown in Figure 5.8. As can be seen, the results for the finite element investigation and the Airbus fatigue model lead to the same behavior. The values only differ some percentages between the two models, however, the fatigue model leads to higher (most conservative results).

Another output of the Airbus fatigue model are maximum bore hole stresses. Based on these stresses, the fatigue life of the repair can be determined, see Figure 5.9. Using these stresses and the Airbus internal fatigue tool, a fatigue life of an unfactored fatigue life of 2 032 978 Flight Cycles is found.

Outcome Fatigue Repair Model - Test case 1													
r\c	1	2	3	4	5	6	7	8	9	10	11	12	13
1	1367	1024	921	816	765	651	502	376	186	153	102	306	605
2	1059	804	536	402	325	301	204	115	76	123	231	422	798
3	1001	716	482	376	301	265	146	96	82	142	242	452	842
4	981	603	432	342	276	212	119	66	94	164	256	477	887
5	941	578	466	436						152	276	486	921
6	902	506	442	562						168	242	432	842
7	882	464	423	623						427	318	442	847
8	847	442	318	427						623	423	464	883
9	842	432	242	168						562	442	506	902
10	922	486	276	152						436	468	579	941
11	867	476	256	164	94	66	119	212	276	342	432	604	981
12	842	452	242	143	82	96	146	265	301	376	482	716	1001
13	798	422	231	123	76	116	204	301	325	402	536	804	1059
14	604	308	102	153	186	376	502	651	765	816	921	1024	1368

Outcome Finite Element Model - Test case 1													
r\c	1	2	3	4	5	6	7	8	9	10	11	12	13
1	1326	1004	939	816	750	625	482	368	179	150	102	312	629
2	1017	764	557	394	315	292	200	112	74	120	226	422	822
3	941	666	482	368	292	257	143	93	80	135	247	443	842
4	903	567	423	332	270	206	117	64	92	159	259	463	841
5	885	543	452	436						147	273	457	884
6	866	476	433	568						168	240	406	800
7	864	445	402	629						436	305	424	839
8	839	424	305	436						629	402	445	865
9	800	406	240	168						568	433	476	866
10	885	457	273	147						436	452	544	885
11	841	462	259	159	92	65	115	208	270	332	423	568	903
12	842	443	247	136	80	93	143	257	292	368	482	666	941
13	822	422	226	120	74	112	200	292	315	394	557	764	1017
14	628	312	102	150	179	368	482	625	750	816	939	1004	1327

Figure 5.8: Transferred forces outcome for the Airbus Fatigue model and the finite element model for test case 1

Max Bore Hole Stress [MPa] Test Case 1							
r\c	7	8	9	10	11	12	13
8				242			
9				216			
10				196			
11	189	194	179	161			
12							
13							
14							222

Figure 5.9: Maximum bore hole stresses for test case 1

5.2.2 Test case 2 - Combined mechanical and thermal

The second test case covers a stiffer aluminium repair under a thermal loading. The parameters for this test case are described in Table 5.2. Using Equation 5.7, a Load Increase Factor of 1.21 is found.

Table 5.2: Overview of the inputs used for test case 2

Parameter	Unit	Value
Cut-Out Size	[mm]	100 x 100
Doubler Size	[mm]	283.6 x 270.85
Skin Size	[mm]	425 x 406
Fastener Pitch	[mm]	4D (≈19.2mm)
Doubler Thickness	[mm]	2.4
Doubler Stiffness	[MPa]	65500
Skin Lay-Up	[-]	4/4/4/4 (≈2.0mm)
Skin Stiffness	[MPa]	57593.1
Skin Loading σ_x / σ_y / τ_{xy}	[MPa]	60 / 40 / 20
Stringer Loading	[MPa]	30
Temperature Loading	[°C]	-38

The results for the transferred forces found using the fatigue repair model and the finite element investigation can be found in Figure 5.10. Here a small discrepancy between the two models is noticed. For the highest transferred forces, a difference of 10% is noticed. This

means that the repair model gives more conservative results than the forces found within the finite element investigation. The mismatch can be explained in the way of how the thermal effect is modelled. Within the Airbus fatigue model, the thermal effect is mainly concentrated in the corners of the repair resulting to higher transferred forces.

Outcome Fatigue Repair Model - Test case 2

r\c	1	2	3	4	5	6	7	8	9	10	11	12	13
1	2160	1597	921	816	765	651	502	376	186	153	102	496	972
2	1684	1206	536	402	325	301	204	115	76	123	231	680	1277
3	1612	1153	482	376	301	265	146	96	82	143	242	732	1347
4	1589	977	432	342	276	212	119	66	94	164	256	762	1379
5	1496	913	466	436						152	276	768	1448
6	1434	799	442	562						168	242	683	1339
7	1402	733	423	623						427	318	712	1372
8	1372	712	318	427						623	423	733	1402
9	1339	683	242	168						562	442	799	1434
10	1448	768	276	152						435	465	913	1496
11	1379	762	256	164	94	66	119	212	277	342	432	977	1589
12	1347	732	242	143	82	96	146	265	302	376	482	1153	1612
13	1277	680	231	123	76	115	204	301	325	402	536	1286	1684
14	972	496	102	153	186	376	502	651	766	815	921	1597	2160

Outcome Finite Element Model - Test case 2

r\c	1	2	3	4	5	6	7	8	9	10	11	12	13
1	1928	1426	873	751	693	581	448	339	166	138	95	456	913
2	1457	1137	513	363	290	271	186	104	70	110	209	620	1199
3	1365	997	448	339	271	237	130	86	75	125	223	660	1253
4	1331	836	390	305	251	191	107	60	85	145	236	680	1244
5	1281	790	416	401						136	249	664	1292
6	1254	692	407	522						155	216	591	1183
7	1252	641	370	579						401	281	622	1263
8	1263	622	281	401						579	370	641	1252
9	1183	591	216	155						522	407	692	1254
10	1292	664	249	136						401	416	790	1281
11	1243	680	236	146	85	60	107	192	251	305	390	636	1331
12	1252	660	223	125	75	86	132	237	271	339	448	997	1365
13	1199	620	208	110	69	103	184	271	290	363	514	1137	1457
14	913	456	94	138	166	339	448	581	683	751	873	1426	1930

Figure 5.10: Transferred forces outcome for the Airbus Fatigue model and the finite element model for test case 2

Regarding the fatigue life, see Figure 5.11, it can be seen that adding the thermal effect and increasing the stiffness of the repair results in higher maximum bore hole stresses, and thus a lower fatigue life. For this configuration, the unfactorised fatigue life is 258 192 flight cycles, which is almost 90% lower than the fatigue life of test case 1.

Max Bore Hole Stress [MPa]
Test Case 2

r\c	7	8	9	10	11	12	13
8				284			
9				269			
10				250			
11	170	168	159	235			
12							
13							
14							379

Figure 5.11: Maximum bore hole stresses for test case 2

5.2.3 Test case 3 - Medium cut-out size with combined loading

The third case has a complete different set-up. It has a medium cut-out size (150 by 150mm) with a maximum fastener pitch in logitudinal direction. The repair is loaded with a thermal load of -58°C. All inputs are summarised in Table 5.3 and the LIF (determined using Equation 5.7) equals 1.38.

Table 5.3: Overview of the inputs used for test case 3

Parameter	Unit	Value
Cut-Out Size	[mm]	150 x 150
Doubler Size	[mm]	333.6 x 395.5
Skin Size	[mm]	500 x 600
Fastener Pitch	[mm]	4D (≈19.2mm)
Doubler Thickness	[mm]	1.8
Doubler Stiffness	[MPa]	65500
Skin Lay-Up	[-]	2/4/4/5 (≈1.9mm)
Skin Stiffness	[MPa]	67879
Skin Loading σ_x / σ_y / τ_{xy}	[MPa]	67 / 86 / 22
Stringer Loading	[MPa]	30
Temperature Loading	[°C]	-58

From Figure 5.12, the difference in transferred forces for the fatigue repair model and the finite element model can be seen. It is noticed that at the corner fastener the difference is around 15%. Another observation which is made is that the fastener forces within the finite element model around the cut-out are much larger. This can be explained by the higher local bending within the finite element model. The second output, Figure 5.13, shows the maximum bore hole stresses for the right under part of the model. Using these stresses together with the Airbus internal fatigue tool, an unfactored fatigue life of 53 711 Flight Cycles is found.

Outcome Fatigue Repair Model - Test case 3

r\c	1	2	3	4	5	6	7	8	9	10	11	12	13	14	15	16
1	3609	2673	2284	2115	2020	1955	1910	1871	1819	1806	1778	1759	1760	1831	2091	2804
2	2888	1828	2746	1173	1078	1029	995	971	943	934	922	926	969	1108	1469	2331
3	2627	1577	1100	866	738	659	604	565	527	519	516	559	669	892	1323	2232
4	2479	1499	1039	819	695	585	486	397	318	262	271	369	555	697	1309	2239
5	2463	1478	1053	930									578	855	1332	2275
6	2405	1463	1047	939									767	943	1371	2316
7	2370	1226	1016	889									857	994	1407	2354
8	2354	1407	994	857									889	1016	1226	2370
9	2316	1371	943	767									939	1047	1463	2405
10	2275	1332	855	578									930	1053	1478	2463
11	2239	1309	697	555	369	271	262	318	397	486	585	695	819	1039	1499	2453
12	2232	1323	892	669	559	518	519	527	565	604	659	738	866	1100	1577	2627
13	2331	1469	1109	969	926	922	934	943	971	995	1029	1078	1173	2746	1828	2888
14	2804	2091	1831	1760	1759	1778	1808	1819	1871	1910	1955	2020	2115	2284	2673	3609

Outcome Finite Element Model - Test case 3

r\c	1	2	3	4	5	6	7	8	9	10	11	12	13	14	15	16
1	3141	2777	2565	2245	2108	1980	1831	1608	1471	1204	1240	1263	1321	1452	1770	2108
2	2906	2266	1904	1713	1542	1465	1392	1253	1279	1343	1380	1387	1419	1542	1881	2267
3	2582	1908	1690	1504	1338	1285	1234	1098	1157	1213	1275	1329	1388	1527	1839	2299
4	2550	1938	1667	1467	1291	1213	1140	1004	930	1001	1157	1215	1414	1553	1895	2310
5	2498	1923	1673	1456									1395	1551	1890	2334
6	2443	1905	1638	1458									1360	1563	1884	2354
7	2400	1800	1530	1362									1302	1480	1762	2381
8	2381	1762	1480	1302									1361	1530	1800	2400
9	2354	1884	1563	1360									1458	1639	1905	2443
10	2334	1891	1550	1395									1456	1674	1923	2498
11	2310	1894	1553	1413	1215	1157	1001	930	1004	1142	1213	1290	1467	1666	1938	2550
12	2299	1839	1527	1389	1329	1275	1213	1157	1098	1233	1285	1338	1504	1690	1988	2582
13	2266	1881	1542	1419	1387	1380	1343	1279	1252	1391	1464	1542	1713	1904	2266	2906
14	2108	1771	1452	1321	1263	1240	1204	1471	1608	1831	1980	2108	2245	2565	2778	3142

Figure 5.12: Transferred forcesouitcome for the Airbus Fatigue model and the finite element model for test case 3

Max Bore Hole Stress [MPa]
Test Case 3

r\c	9	10	11	12	13	14	15	16
8					365			
9					373			
10					366			
11	302	311	316	318	324			
12								
13								
14								503

Figure 5.13: Maximum bore hole stresses for test case 3

5.3 Conclusion

Based on the correlations which were found in the finite element study and which were confirmed using the Airbus internal models, it is shown that an analytical equation can be set-up for estimating the load transfer. This analytical equation has been tested using three cases, where the Load Increase Factor was applied on the Airbus internal fatigue model and the outcome has been compared to the finite element model (possiblility to model stringer). For the analysed cases, a correlation was found, though the Airbus fatigue model always lead to more conservative results than were found using the finite element solution.

The last step is to determine the validity range of this simplified equation. Since only a limited number of test cases has been checked. The validity range for this equation is:

- Aluminium doublers made of Al2024Clad-T3 in full thickness range for repairs
- For all configurations with a stiffness ratio between 0.8 and 1.4
- For all negative thermal loadings
- For cut-out sizes up to 150 by 150mm
- For all configurations with four rivet rows or more around the cut-out
- For all rivet pitches between 4D and 6D

Another advantage of using the Airbus tool is the possibility to extract bore hole stresses, which allow to directly calculate the fatigue life and the fact that this module was already used for the justification of metallic repairs on metallic fuselages.

Chapter 6

Conclusions and Recommendations

Conclusions

The goal of this thesis was to research the load transfer capability of a hybrid doubler repair configuration using different tools, which were a finite element model and internal Airbus models.

First, a finite element model was created with Abaqus and a parametric study was conducted to see the effect of the load transfer of the present stiffening structure on the repair. Here it was seen that a change of material of the repair patches (sized on iso-stiffness) lead to large differences in the load transfer capability of the repair. A second observation was that increasing the stringer loading resulted in an increase of the load transfer. A large influence of the thermal stresses on the behavior of the hybrid repair was found. The highest negative temperature difference had the largest effect on the load carrying capability of the model. Therefor the repair justification should be performed using a realistic value for the temperature of the skin at that bay and not with a conservative temperature difference as was done in the past by Airbus. Here it was also seen that changing the number of rivet rows, or changing the fastener pitch, mainly affects the load re-distribution and only changes slightly the load transfer. Regarding this load transfer, the finite element investigation showed that only the longitudinal loading is affected. Therefor, a Load Increase Factor should be applied only on the longitudinal loading component.

The behavior of the finite element model for the different parameters was compared to different Airbus internal tools which are simplified models able to perform load transfer calculations. It was seen that the two-dimensional Airbus model shows the best match with the results of the Load Increase Factor. The other models (simple one-dimensioonal stripe models bolted and bonded & and complex one-dimensional stripe model) lead to higher more conservative results. The analytical equation which is only based on fluxes and stiffness ratio shows a bad match with all other models.

Based on the correlations which were found in the finite element study and which were confirmed using the Airbus internal models, it is shown that an analytical equation can be set-up for estimating the load transfer. This analytical equation has been tested using three cases, where the Load Increase Factor was applied on the Airbus internal fatigue model. This model has no possiblity to model stringer, so a Load Increase Factor should be applied. The outcome has been compared to the finite element model, where it is possible to model the stringer. For the analysed cases, a good correlation was found though the Airbus fatigue model always lead to more conservative results than those using the finite element solution.

Recommondations

In this last part, several recommendations will be given to improve the parametrical equation, based on the finite element investigation.

First of all, all results are obtained by comparing models and no complete verification could be done due to the lack of test results with temperature loading. Therefor, a panel test should be performed under varibale temperature conditions to determine the load transfer from the panel to the repair together with the most critical location. Using these test results, the analytical equation can be finetuned.

A second improvement is an increase of the validity range of this analytical equation. A comparison between the Airbus fatigue model and the finite element model should still be performed for

- different materials, such as Titanium and CFRP-doublers for different thickness ranges.
- stiffness ratio's with an Aluminium doubler higher than 1.4
- cut-out sizes larger than 150 by 150mm.
- a configuration with three rivet rows.
- repairs over frames.
- repairs with a T-stringer configuration.

Appendices

Appendix A

Non-Disclosure Agreement

This appendix contains the non-disclosure agreement which was signed between Airbus GmbH and Delft University of Technology.

AIRBUS
AN EADS COMPANY

Non-Disclosure Agreement

1. The entire / the marked part of the final thesis of:

   Mr. Florian Vandenberk

   contains confidential data of Airbus Operations GmbH which may only be used for the issue of the final thesis and the conjoint examination procedures.

   The contents of the thesis may only be made accessible to the supervisors and the members of the examination office.

   The use of the thesis particularly as part of lectures is not allowed without written consent of the Airbus Operations GmbH.

2. Confidential information shall not, either as a whole or in part, be published, reproduced or disclosed to a third party unless the express written consent of Airbus Operations GmbH has been obtained.

3. Secrecy shall be observed in regard to all corporate matters and operations of Airbus Operations GmbH and its affiliated companies which are not publicly known and of which knowledge is obtained by tutoring the student – in written or oral form – either from the student or from Airbus Operations GmbH itself.

4. The declaration of secrecy shall enter into force once this agreement has been signed and shall remain valid for 3 years.

Technical University Delft

Place, date Delft, 2-12-2013

Signature

(On behalf of Technical University Delft)

Prof. dr. ir. H. Bijl

Appendix B

Determination of Load Transfer using Stripe Models

This appendix describes how the Load Increase Factor is derived from using simplified stripe models. These models help to estimate the load transfer between a model with and without stringer. Figure B.1 shows a cross-section of a typical skin repair with doubler.

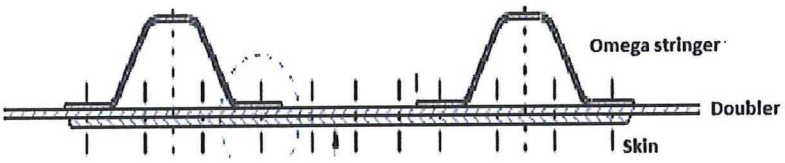

Figure B.1: Process of Simplification

Loads acting on the model The model should be loaded with the longitudinal skin loading (σ_x), stringer load ($\sigma_{stringer}$) and temperature difference (ΔT).

Modelling Two models should be created, namely:

- **Model 1:** Stripe model representing repair, skin and stringer foot with longitudinal skin load, stringer load and temperature difference. Here, a bondline can be included in the model, see Model 1 in Figure B.2.
- **Model 2:** Stripe model representing repair and skin, which is loaded with the longitudinal skin load and temperature difference, see Model 2 in Figure B.2.

The output of both models are the transferred forces for each fastener.

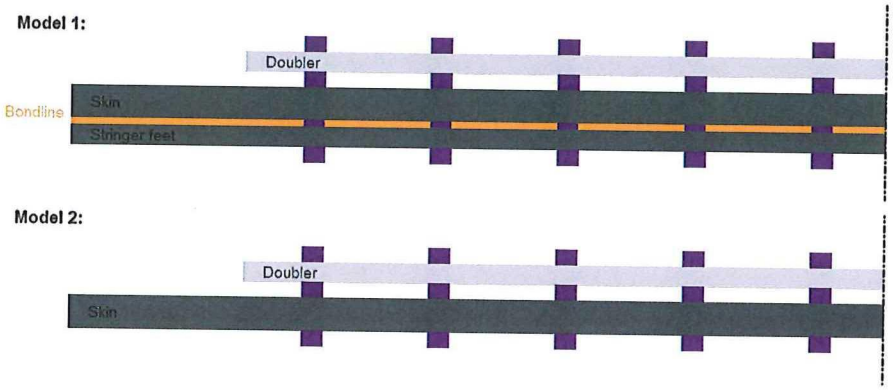

Figure B.2: Overview of used stripe models

Determing Load Increase Factor The Load Increase Factor is determined as the factor which need to be applied to get on the skin longitudinal stress component of model 2 the same transferred load as was found for model 1. To avoid a time-consuming iterative process, a simpler process can be applied. This is done by running the second model with different values of the longitudinal skin load component, multiplied for different Load Increase Factors, as is illustrated in Figure B.3. Using this approach, the LIF can be determined, without applying a long iterative process.

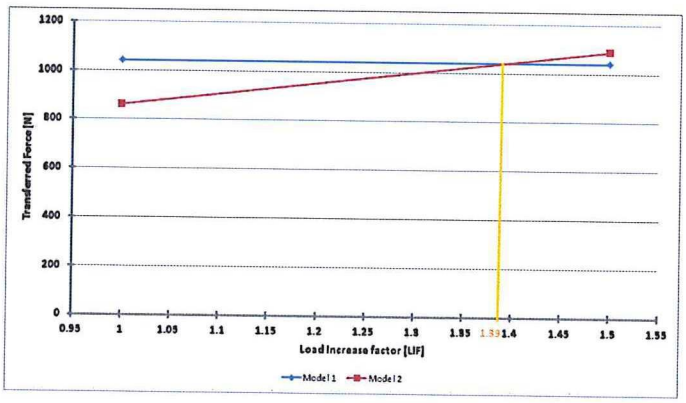

Figure B.3: Overview of graph to calculate LIF for simplified Airbus model

This LIF is now applied on the longitudinal component within the repair model for fatigue calculations, see Appendix C.

Appendix C

Airbus Repair Model

This appendix describes the main characteristics of the Airbus internal fatigue model. It is a simplified model to calculate the fatigue life of a repair and it was designed for legacy aircraft, which means aircraft with a metallic fuselage and metallic repairs. The model was adopted to handle hybrid repairs (composite skin materials with metallic doublers). It creates a local finite element model of the skin with cut-out and a doubler. One of the main limitations is that the stringer cannot be modelled. For the legacy aircraft, this was no problem since the load transfer from the stringer to the repair could be neglected.

The plates can only be joined by fasteners. This model is specifically designed to handle fatigue calculations, though it is not coupled to a spectrum calculation, since this would cost to much calculation time. Therefor the model is loaded with a fatigue reference load case which can include a thermal effect. The model is solved unstabilised, permitting secondary bending effects. Other inputs for this model are the skin properties (material, lay-up or thickness and size), doubler properties (material, thickness and size), cut-out properties (length, width and corner radius), loading (longitudinal, circumferential and shear) and the thermal loading. Also a detailed fastener pattern is part of the input.

This model has three main outcomes, namely:

- transferred force of each fastener.
- maximum principle stress in the middle of the doubler.
- maximum bore hole stresses of each fastener.

The model can be runned with a simplified fastener and a three-dimensional equivalent:

- A **simplified fastener** is a connecting element modelled with the shear flexibility defined by the Huth-equation, see Equation C.1, and elongation stiffness given by Equation C.2 which gives transferred forces.

$$C = \frac{t_1 + t_2}{2 \cdot d}^{a} \cdot \left(\frac{b_1}{t_1 \cdot E_1} + \frac{b_2}{t_2 \cdot E_2} + \frac{b_1}{2 \cdot t_1 \cdot E_3} + \frac{b_2}{2 \cdot t_2 \cdot E_3} \right) \tag{C.1}$$

Where:

- C = Flexibility of the fastener
- t_1 = Thickness of plate 1
- t_2 = thickness of plate 2
- E_1 = Young modulus of plate 1
- E_2 = Young modulus of plate 2
- E_3 = Young modulus of the fastener
- a = Coefficient depending on the fastener type
- b_1, b_2 = Coefficients depending on the joint plates

$$K = \frac{E \cdot S}{L} \tag{C.2}$$

Where:

- E = Young modulus of the fastener
- S = Section area of the fastener
- L = Length of the fastener

- A **three-dimensional fastener** is modelled as a three dimensional solid element which takes into account the local deformation of the fastener. For this element, the stresses at different angles of the bore hole are calculated.

Adding extra three dimensional fasteners refine the calculation results, however jeopardises the calculation time.

The maximum bore hole stresses can be directly used to determine the fatigue life of the analysed configuration. The model is only able to perform metallic fatigue calcualtions, this means that the fatigue characteristics of the doubler need to be checked in a different way.

References

[1] Abaqus - Simulia, *Abaqus 6.13 Manual.*

[2] Airbus, http://www.airbus.com/work/why-join-airbus/training-and-development/composites-manufacturing-assembly/, *Last visited: 12/10/2014.*

[3] Airbus, *New service packages will extend A320s life* http://www.airbus.com/presscentre/pressreleases/press-release-detail/detail/new-service-package-will-extend-a320039s-life/, *Last visited: 12/10/2014.*

[4] Anderson, J.D., *Introduction to Flight.* McGraw-Hill Education, 7th edition, 2011.

[5] Barsom, J.M. and Rolfe, S., *Fracture and Fatigue Control in Structures. Applications of Fracture Mechanics.* Butterworth-Heinemann, 3rd edition, 1999.

[6] Bold, J., *Airbus Composite Training.* VPD Conference Frankfurt, 17/10/2007, http://web.mscsoftware.com/events/vpd2007/emea/presentations/Session-2A-AIRBUS-Bold.pdf.

[7] Forrest, P., *Fatigue of Metals.* Pergamon Press Oxford, 1st edition, 1962

[8] Gramoll, K., *ECourse Mechanics - Chapter 6: Advanced Beams.* http://www.ecourses.ou.edu/cgi-bin/ebook.cgi?doc=&topic=me&chap_sec=06.1&page=theory Last visited on 19/12/2014.

[9] Hagenbeek, M., *Characterisation of Fibre Metal Laminates under Thermo-Mechanical Loadings.* Phd. Thesis, 1st edition, 2005

[10] Hibbeler, R.C., *Mechanics of Materials*, Prentice Hall, 9th edition, 2014.

[11] Kassapoglou, C., *Design and Analysis of Composite Structures: With Applications to Aerospace Structures.* Aerospace Series, Wiley, 2nd edition, 2013.

[12] Kassapoglou, C., *Predicting the Structural Performance of Composite Structures Under Cycling Loading.* PhD Thesis, Delft University of Technology, 2012.

[13] Laulusa et al., *Evaluation of some shear deformable shell elements.* http://soliton.ae.gatech.edu/people/obauchau/publications/Laulusa+Bauchau+Choi+Tan+%20Li06.pdf, Last visited: 08/10/2014.

[14] International Agency for Research on Cancer (IARC), *IARC Monographs on the Evaluation of Carcinogenic Risks to Humans, Man-made Vitreous Fibres, Summary of Data Reported and Evaluation.* World Health Organisation, Volume 81, 2002.

[15] Lovatt A., Shercliff H., http://www-materials.eng.cam.ac.uk/mpsite/interactive_charts/hardcopy/B&W/Stiffness-Density/, *Last visited: 07/10/2014.*

[16] Lovatt A., Shercliff H., http://www-materials.eng.cam.ac.uk/mpsite/interactive_charts/hardcopy/B&W/Strength-Density/, *Last visited: 07/10/2014.*

[17] Megson, *Aircraft Structures for Engineering Students.* Elsevier, Aerospace Engineering Series, 4th edition, 2007.

[18] Navy Aviation, *Aviation Structural Mechanic (H & S) 3 & 2 - How airplanes are built and how to maintain them.* http://navyaviation.tpub.com/14018/index.htm, *Last visited on 07/10/2014.*

[19] Niu, M.C.Y., *Composite airframe structures: practical design information and data.* Conmilit Press, 3rd edition, 2000.

[20] Niu, M.C.Y., *Airframe Stress Analysis and Sizing.* 2nd edition, 2011.

[21] Niu, M.C.Y., *Composite airframe structures: practical design information and data.* Conmilit Press, 3rd edition, 2000.

[22] Shen, C., Springer S.G., *Environmental Effects on the Elastic Moduli of Composite Materials.* Journal of Composite Materials, Vol. 11, 1977, pp. 250-264.

[23] Shen, C., Springer S.G., *Effects of Moisture and Temperature on the Tensile Strength of Composite Materials.* Journal of Composite Materials, Vol. 11, 1977, pp. 2-15.

[24] Schultheisz, R.C. et al., *Effect of Moisture on E-Glass/Epoxy Interfacial and Fiber Strengths.* Composite Materials: Testing and Design, ASTM STP 1242, Vol. 13, 1997, pp. 257-286.

[25] Schijve, J., *Fatigue of Structures and Materials.* Springer, 2nd edition, 2008.

[26] University of Colorado at Boulder, *Introduction to Finite Element Methods.* Lecture Series, Fall 2014, http://www.colorado.edu/engineering/cas/courses.d/IFEM.d/.

[27] WrightStories.Com, *"Celebrate The Success Of The Wright Brothers" - The first attempt.* http://www.wrightstories.com/kittyhawk.html, *Last visited on 17/11/2014.*